DOI:10.14753/SE.2025.3134

SEMMELWEIS EGYETEM

DOKTORI ISKOLA

Ph.D. értekezések

3134.

BÁTAI BENCE

Onkológia

című program

Programvezető: Dr. Bödör Csaba, egyetemi tanár

Témavezető: Dr. Bödör Csaba, egyetemi tanár

DOI:10.14753/SE.2025.3134

INVESTIGATION OF SPATIAL AND TEMPORAL HETEROGENEITY IN THE GENETIC BACKGROUND OF GERMINAL CENTER LYMPHOMAS

PhD thesis

Bence Bátai, MD

Doctoral School of Pathology

Semmelweis University

Supervisor: Csaba Bödör, DSc

Official reviewers: Zoltán Wiener, DSc
Ferenc Magyari, MD, PhD

Head of the Complex Examination Committee:
Judit Demeter, MD, DSc
Members of the Complex Examination Committee:
Janina Kulka, MD, DSc
Erika Tóth, MD, PhD

Budapest
2024

DOI:10.14753/SE.2025.3134

TABLE OF CONTENTS

DOI:10.14753/SE.2025.3134

DOI:10.14753/SE.2025.3134

LIST OF ABBREVIATIONS

AID: activation-induced cytidine deaminase

ARID1A: AT-rich interaction domain 1A

BCL2: B-cell leukemia/lymphoma 2

BCL6: B-cell leukemia/lymphoma 6

BCR: B cell receptor

BTK: Bruton's tyrosine kinase

CARD11: caspase recruitment domain-containing protein 11

CAR-T: chimeric antigen receptor T-cells

CDK4: cyclin dependent kinase 4

CDKN2A: cyclin-dependent kinase inhibitor 2A

CDKN2B: cyclin-dependent kinase inhibitor 2B

cfDNA: cell-free DNA

CNA: copy number alteration

CT: computed tomography

ctDNA: circulating tumor DNA

CR: complete response

CREBBP: CREB binding protein

ddPCR: digital droplet PCR

dFL: diffuse follicular lymphoma

DLBCL: diffuse large B-cell lymphoma

aEFS: event free survival

EORTC: European Organization for Research and Treatment of Cancer

EP300: histone acetyltransferase p300

ESMO: European Society of Medical Oncology

EZH2: Enhancer of zeste homolog 2

fDC: follicular dendritic cells

FFPE: formalin fixed, paraffin embedded

FL: follicular lymphoma

ctFLIPI: follicular lymphoma international prognostic index

FISH: fluorescent in situ hybridization

FOXO1: forkhead box protein O1

GC: germinal center

GCB: germinal center B cell

GELF: Groupe d'Etude des Lymphomes Folliculaires

IGH: immunoglobulin heavy chain

IQR: interquartile range

KMT2D: lysine methyltransferase 2D

LDH: lactate dehydrogenase

MAP2K1: mitogen-activated protein kinase kinase 1

MEF2B: myocyte enhancer factor 2B

MTOR: mammalian target of rapamycin

NGS: next-generation sequencing

NHL: non-Hodgkin lymphomaNR: no response

PCFCL: primary cutaneous follicle center lymphoma

PCMZL: primary cutaneous marginal zone lymphoma

PCR: polymerase chain reaction

PET: 18-fluorodeoxyglucose positron emission tomography

PFS: progression free survival

POD24: progression of disease within 24 months

PR: partial response

R-CHOP: rituximab, cyclophosphamide, doxorubicin, vincristine, prednisone

R-CVP: rituximab, cyclophosphamide, vincristine, prednisone

R/R: relapsed/refractory

STAT6: signal transducer and activator of transcription 6

TFH: T follicular helper cells

tisDNA: tissue DNA

TNFAIP3: TNF alpha induced protein 3

TNFRSF14: tumor necrosis factor receptor superfamily member 14

XPO1: exportin 1

WHO4R: Revised fourth edition of World Health Organization Classification for Haematolymphoid Tumors

WHO5: Fifth Edition of the World Health Organization Classification for Haematolymphoid Tumors

DOI:10.14753/SE.2025.3134

1. INTRODUCTION

B-cell non-Hodgkin lymphomas (NHL) are the most prevalent lymphoid malignancies in adult patients, with an estimated 20 new diagnoses per 100 000 inhabitants per year in developed countries (1). Understanding the heterogeneity of this disease group through molecular studies including the investigation of genetic, transcriptional and expression changes have improved current diagnostic classification, risk stratification and therapeutic decision making (2). Although the outcome of B-cell NHL-s has improved during the past two decades due to the approval of anti-CD20 antibodies, the development of relapsed/refractory disease, as well as tailoring treatment intensity to avoid unnecessary toxicity are unmet needs of clinical management in most subtypes, warranting further research to understand the biological determinants of disease progression and response to therapy.

This thesis focuses on the genetic background of a rare B-cell lymphoma subtype, primary cutaneous follicle center lymphoma (PCFCL) and the most prevalent indolent lymphoma subtype, follicular lymphoma (FL). Diagnosis and management of PCFCL is historically defined in comparison with FL, therefore in the introduction we will first discuss the diagnosis and management of FL then we will highlight special aspects about the diagnosis and management of PCFCL.

1.1 DIAGNOSIS AND MANAGEMENT OF FOLLICULAR LYMPHOMA

1.1.1. Clinical presentation and diagnostic workup

Follicular lymphoma is the most common indolent NHL accounting for about 15-20% of malignant B-cell lymphomas (3). Median age at diagnosis is between 60 and 70 years, and its incidence and prevalence are expected to increase as life expectancy continues to increase and diagnostic and therapeutic techniques show further improvement.

Follicular lymphoma most commonly presents with painless, progressive lymphadenopathy. Deep lymph nodes may also be involved, with the retroperitoneal and mesenteric sites being most commonly affected, occasionally resulting in local symptoms of compression or infiltration of adjacent organs. A minority of cases are characterized by an extranodal appearance, which may involve any organ system, such as the gastrointestinal system, skin, skeletal muscle or fallopian tubes (4). Later, the appearance of systemic symptoms, so called "B" symptoms including fever, night sweats or weight

loss can follow. Diagnosis of follicular lymphoma is warranted based on the history, physical examination of the lymphoreticular and haematopoietic systems, blood counts, imaging and can be confirmed using pathological examination of the involved tissue specimens. Based on the current guideline of the European Society of Medical Oncology (ESMO) diagnostic workup should include computed tomography (CT) scans of the neck, chest, abdomen to determine the extent of the disease, while 18-fluorodeoxyglucose positron emission tomography-CT (PET-CT) is the recommended imaging modality for staging, with high-level evidence recommending its usage in localised disease and suspected transformation (5). A definitive pathological diagnosis may be made depending on the results of histological and cytological examination detailed below. Diagnostic workup should also include bone marrow biopsy with flow cytometry examination of the bone marrow to exclude bone marrow infiltration. Occasionally, polymerase chain reaction (PCR) testing for BCL2 gene rearrangements may help to confirm the diagnosis (5).

1.1.2. Pathological diagnosis

In follicular lymphoma, excision sampling of the infiltrated lymph node or bone marrow biopsy is preferably performed to obtain a histological sample (6). The histological picture of follicular lymphoma in the majority of cases shows a follicular growth pattern, composed of centrocytes and centroblasts, and the lesion also contains reactive centrum germinativum specific T cells and antigen-presenting follicular dendritic cells. Histological grading is now optional based on the recently published fifth edition of the World Health Organization Classification for Haematolymphoid Tumors (WHO5) (2), but until lately has been performed based on the number of centroblasts and remaining to be used in the research setting: <5 centroblasts per high-power field corresponds to grade I disease, 6-15 centroblasts per high-power field to grade II disease, 15< centroblasts per high-power field to grade III disease. Disease with grade III histology is classified as follicular large B-cell lymphoma or previously called grade IIIB FL with contiguous centroblast areas and grade IIIA with no contiguous centroblast areas (2, 7).

Immunohistochemical testing with antibodies against CD20, CD3, CD5, CD10, BCL2, BCL6, CD21, and CD23 is essential for histopathological diagnosis according to the National Comprehensive Cancer Network recommendation on B-cell lymphomas (8). Follicular lymphoma is characterized by CD10+, BCL2+, CD23+/-, CD5-, CD20+,

BCL6+ immunophenotypes, but BCL2- and CD10- cases also occur. The extent of proliferation can be assessed by immunohistochemistry against Ki67.

Flow cytometry is recommended to examine kappa/lambda light chain, CD19, CD20, CD5, CD23, and CD10 surface markers (8).

Karyotyping or FISH can be used to identify the presence of t(14;18) translocation, BCL6 rearrangement, IRF4/MUM1 fusion gene, and 1p36 deletion in the tumor sample. The t(14;18) translocation is not specific for follicular lymphoma, but is present in the majority of cases and may help in differential diagnosis. The 1p36 deletion is particularly common in diffuse follicular lymphoma (dFL, WHO5) of the inguinal or pelvic region, showing diffuse growth pattern and CD23 positivity, while being *BCL2* rearrangement negative (8).

1.1.3. Prognosis and treatment

FL is an indolent disease, with 5-year overall survival (OS) rates reaching 75% since the approval of rituximab therapy (9). Prediction of progression of disease within 24 months (POD24) is particularly important in FL, as the development of relapse within 2 years results in shorter OS (5-year OS 50% vs. 90%) (10). Transformation to diffuse large B-cell lymphoma (DLBCL) occurs in about 2-3% of cases per year conferring poor prognosis (11-13). Clinically, rapid lymph node growth, abnormally high LDH, rapid deterioration of ECOG status, development of "B" symptoms, hypercalcemia, and dissemination to extranodal areas may indicate the development of transformed FL. Confirmatory histopathology is always recommended in suspected cases showing the disappearance of follicular structure and the development of high-grade histology (14, 15).

Several prognostic models have been developed for follicular lymphoma to estimate the expected course of the disease with the most commonly used being the Follicular Lymphoma International Prognostic Index (FLIPI). Factors considered as poor prognostic factors in the model are age ≥60 years, Ann Arbor stage III-IV, haemoglobin level <12 g/dl, affected lymph node regions >4, and serum LDH concentration above the normal range (16). However, the FLIPI model is not perfect, and several attempts have been made to augment the model to provide more accurate risk stratification. These include the m7-FLIPI clinicogenetic model, which, in addition to the FLIPI and Eastern Cooperative Oncology Group (ECOG) scores, takes into account the mutation status of seven genes

(*EZH2, ARID1A, EP300, FOXO1, MEF2B, CREBBP, CARD11*) in determining prognosis resulting in more accurate risk stratification (17).

Therapeutic approach for follicular lymphoma is based on the stage of the disease, using the Ann Arbor staging system, differentiating patients with limited stage disease (stage I-II) with tumor sites on one side of the diaphragm, or advanced stage disease (stage III-IV) with involved lymph nodes and/or extranodal sites on both sides of the diaphragm (18). Indication for treatment is established using the Groupe d'Etude des Lymphomes Folliculaires Criteria involving the presence of bulky tumor, more than 3 tumor sites, B symptoms, splenic enlargement, compression syndrome, pleural or peritoneal serous effusion, leukemic phase and neutropenia or thrombocytopenia as indications for treatment (19). When considering the therapeutic strategy and the indication for treatment, patients can be divided into 3 groups:

a) approximately 20% of patients have stage I-II disease, which can be potentially cured with irradiation of the affected lymph node region with a total dose of 24 Gy resulting in a 10-year relapse-free survival of 45-60% and a 10-year expected survival of up to 60-80% (20)
b) for asymptomatic follicular lymphoma based on the GELF Criteria with a small tumour mass, "watch and wait" strategy is recommended, as early therapy has not been shown to be effective in either improving survival or preventing transformation, but reduces side effects and the cost of medication (21)
c) for symptomatic disease, combination therapy based on an anti-CD20 antibody - primarily rituximab - is recommended as the primary treatment, optionally followed by rituximab maintenance therapy (8).

FL is characterized by a remitting-relapsing disease course. In the case of limited stage relapse and in the absence of previous radiotherapy, radiotherapy is indicated, while in advanced stage cases, the choice of combination therapies described above is recommended, optimally using another regime that was applied during the previous treatment line (8). Recently, the therapeutic landscape is changing, as a number of targeted therapeutics and immunotherapy agents have been investigated for the treatment of relapsed/refractory (R/R) patients, resulting in the recommendation of EZH2 inhibitor tazemetostat in second line treatment, and tazemetostat, the BTK inhibitor zanubrutinib, mosunetuzumab and epcoritamab bispecific T-cell engagers, and axicabtagene ciloleucel,

lisocabtagene maraleucel and tisagenlecleucel CD19 directed CAR-T cells in third line treatment, although with a limited availability in Hungary (8).

1.2. DIAGNOSIS AND MANAGEMENT OF PRIMARY CUTANEOUS FOLLICLE CENTER LYMPHOMA

1.2.1. Clinical presentation and diagnostic workup

PCFCL most commonly involves the head and neck region or the trunk with solitary or multiple lesions. The lesions may vary in appearance and may be erythematous plaques, papules or nodules, which are often itchy and painful. The disease is rarely disseminated and therefore systemic symptoms are not common. The prognosis of primary cutaneous follicular lymphoma is excellent, with a 5-year OS over 95% (22). Differentiating between PCFCL and secondary cutaneous involvement of FL can be a major diagnostic challenge, especially in cases where systemic disease presents with local skin lesions. A diagnosis of primary cutaneous follicular lymphoma can only be made if there is no extracutaneous involvement at the time of diagnosis, based on the diagnostic workup of FL described in detail in the previous section.

1.2.3. Prognosis and treatment

In contrast to FL, PCFCL has an excellent prognosis, with a 5-year OS of more than 95% (23, 24). Despite the low mortality rate, the quality of life of patients can be impaired as a result of high incidence of local recurrences and dissemination of skin lesions to other regions.

Considering potential prognostic factors different disease characteristics were deemed as determinants of prognosis including histological appearance, anatomical localisation of the lesion and the number of lesions, although none of them has become universally accepted (25).

The choice of treatment modality depends on the stage of the disease (Table 1.) (26).

For stage T1 and T2 disease, the choice of local radiotherapy with a dose of 30 Gy is indicated, but surgical resection and intralesional steroid therapy are also considered as alternative therapeutic options, and the possibility of observation may be considered. In cases described in the literature, chemotherapy and chemoradiotherapy are also used (27-29).

For stage T3 disease with generalized skin involvement, topical or systemic rituximab treatment, palliative low-dose local radiotherapy, surgical resection, observation, intralesional steroid therapy, and combined chemoimmunotherapy are among the recommended therapeutic modalities (28, 29). In case of extracutaneous dissemination, combined chemoimmunotherapy is indicated as in FL (29).

Table 1. *TNM classification of cutaneous lymphomas other than mycosis fungoides and Sezary syndrome (26)*

T	
T0	No evidence of clinically suspicious lesion
T1	Solitary lesion
T1a	Solitary <5 cm diameter
T1b	Solitary ≥5 cm diameter
T2	Multiple lesions limited to 1 body region or 2 contiguous body regions
T2a	All disease encompassing in a <15-cm-diameter circular area
T2b	All disease encompassing a 15 to <30 cm diameter circular area
T2c	All disease encompassing a ≥30 cm diameter circular area
T3	Generalized skin involvement
T3a	Multiple lesions involving 2 noncontiguous body regions
T3b	Multiple lesions involving ≥3 body regions
N	
N0	No clinical or pathologic LN involvement
N1	Involvement of 1 peripheral LN region that drains an area of current or prior skin involvement: biopsy positive for lymphoma
N2	Involvement of >2 peripheral LN regionsc or involvement of any LN region that does not drain an area of current or prior skin involvement: biopsy positive for lymphoma
N3	Involvement of central lymph nodes: biopsy positive for lymphoma
Nx	Clinically abnormal peripheral or central LN but no pathologic determination. Other surrogate means of determining involvement may be determined by Tri-Society consensus
M	
M0	No visceral involvement
M1	Visceral involvement
Mx	Visceral involvement is neither confirmed nor refuted by available pathologic or imaging assessment

1.3. PATHOGENESIS OF B-CELL NON-HODGKIN LYMPHOMAS

1.3.1. Germinal center reaction

During their development, B cells undergo several stages in which they become susceptible to malignant transformation. The various B-cell malignancies, leukaemias

DOI:10.14753/SE.2025.3134

and lymphomas, can be traced back to malignant transformation at different stages of the B-cell developmental lineage (Figure 1.).

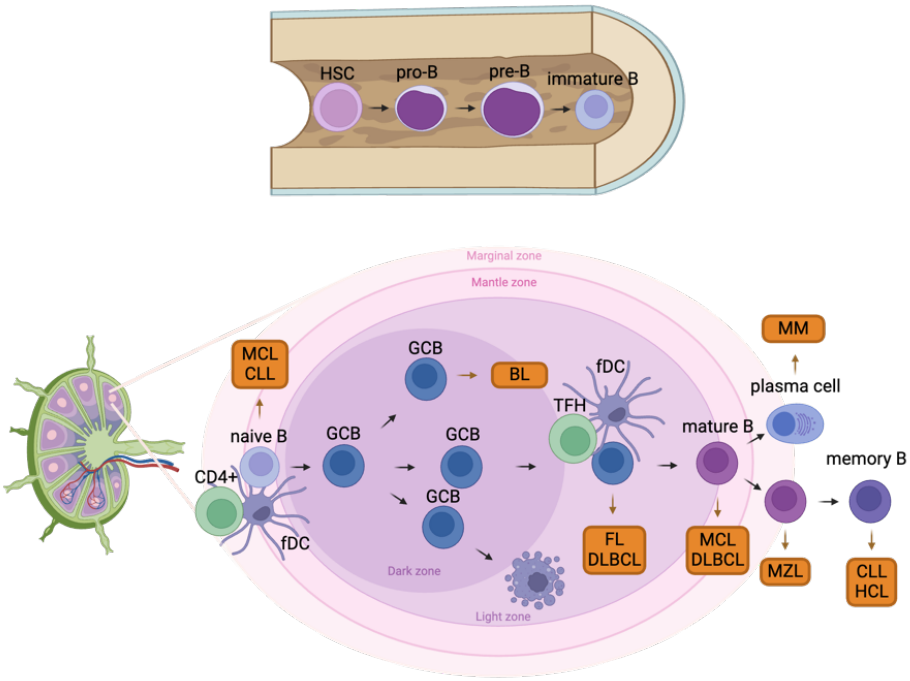

Figure 1. *Schematic overview of B-cell development. Development of B-cells starts in the bone marrow with the development of the B-cell receptor. Antigen naïve B-cells undergo somatic hypermutation and immunoglobulin class switch in the secondary lymphoid organs resulting in increased affinity to exogenous antigens. B-cell maturation is characterized by increased genomic instability prone to development of B-cell lymphomas. Next to cells we depicted lymphoma subtypes originating from the respective maturation stage. Abbreviations: BL: Burkitt lymphoma, CLL: chronic lymphocytic leukemia/lymphoma, DLBCL: diffuse large B-cell lymphoma, FL: follicular lymphoma, HCL: hairy cell leukemia, MCL: mantle cell lymphoma, MM: multiple myeloma, MZL: marginal zone lymphoma*

Like many other non-Hodgkin lymphomas, follicular lymphoma and primary cutaneous follicle center lymphoma are considered germinal center (GC) lymphomas (30). The germinal center reaction plays a major role in the pathogenesis of B-cell lymphomas and can be divided into two zones: the dark zone, composed mainly of centroblasts, characterized by a high mitotic rate and a process of somatic hypermutation, and the light zone, composed of centrocytes undergoing selection for rearranged B-cell receptor affinity and immunoglobulin class switching (31). During the germinal center reaction,

antigen naïve B cells undergo serial division, affinity maturation by somatic hypermutation, receptor revision, and immunoglobulin class switching, leading to the proliferation of B-cells harboring a receptor against a potential target antigen and not inducing autoimmunity (31, 32). The process of somatic hypermutation requires the activity of activation-induced cytidine deaminase, which induces mutations in the variable region of the immunoglobulin gene, and thus develops increased affinity to the antigens bound to the surface of follicular dendritic cells (fDC). Immune synapsis with helper follicular cells (TFH) activates anti-apoptotic signalling pathways in high-affinity clones, allowing them to survive in an apoptosis-promoting environment and continue their differentiation into plasma cells or memory cells.

The GC reaction may result in the activation of oncogenes and inactivation of tumour suppressor genes due to the activity of activation-induced cytidine deaminase,flb in promoting the formation of somatic mutations, leading to malignant transformation of B cells. In addition, the cells do not differentiate further into memory or plasma cells, but re-enter the centrum germinativum reaction, resulting in the accumulation of gene mutations and chromosomal aberrations (33).

1.3.2. Genetic background of germinal center lymphomas

The mapping of the genome of GC lymphomas has revealed that a number of mutations, copy number alterations (CNA) and chromosomal alterations affecting different signalling pathways contribute to the pathogenesis of the disease. Alterations have been observed in genes encoding epigenetic regulatory molecules, BCR signalling pathway molecules, mTOR signalling proteins, B-cell development pathway molecules, proteins responsible for immune regulation, and molecules responsible for apoptosis. Most frequently altered genes and the contribution of the affected molecules to lymphomagenesis in FL and PCFCL are described below.

Mutations affecting epigenetic regulators mainly disrupt post-translational modification of histone proteins, but mutations in histone protein coding genes are also common, leading to epigenetic imbalance (34-36). The *KMT2D* histone methyltransferase acts as a tumour suppressor gene and its loss-of-function mutations, which occur in 80% of FL and 20% of PCFCL cases, result in a reduction in the amount of chromatin signals that activate transcription (37-39). *CREBBP* and *EP300* encode histone acetyltransferases acetylating the lysine residue 27 (H3K27) of histone H3. Inactivating mutations in *CREBBP* are

detected in 60% and 25% of FL and PCFCL patients, respectively, while inactivating mutations in *EP300* were detected in 15% of FL and 18% of PCFCL patients (34, 40). Mutations lead to decreased expression of tumour suppressor genes in the region and genes responsible for exiting the GC reaction, promoting oncogenesis (41). The *EZH2* histone methyltransferase inhibits transcription by methylating the H3K27 side chain playing a key role in maintaining the epigenetic balance. Increased histone methylation inhibits the transcription of tumor suppressor genes due to the gain-of-function mutations that occur in about 25% of FL patients, but rarely detected in PCFCL (40, 42, 43). The clinical relevance of *EZH2* mutations is enhanced by the fact that the gain-of-function mutations make EZH2 a potential therapeutic target and that EZH2 inhibitors have already been approved for the treatment of R/R FL (8, 44).

Alterations of genes encoding B cell receptor (BCR) signaling molecules are predominant in GC lymphomas activating the NF-κB transcription factor. Majority of the BCR pathway is affected by somatic mutations in patients with FL and PCFCL with mutations enriched in *EPHA7*, *TNFAIP3/A20* and *CARD11*, as well as *FOXO1*, but showing differences in prevalence between PCFCL and FL (40). The *FOXO1* transcription factor plays an important role in regulating the transcription of molecules responsible for differentiation, cell cycle regulation, DNA repair and oxidative stress. In FL, gain-of-function mutations in the *FOXO1* gene are found in 5-10% of cases, while in PCFCL in up to 17% of cases (40).

The tumour microenvironment plays a prominent role in the pathogenesis of GC lymphomas. Mutations in the *TNFRSF14* gene, which plays an important role in immune regulation, occur in 28% of FL cases. Additionally, 1p36 deletion also leads to loss of *TNFRSF14*, resulting in the overall inactivation of TNFRSF14 in 50% of patients with FL (45). Decreased expression of the receptor results in reduced inhibitory signalling due to binding to the BTLA receptor, which is present on both TFH cells in the tumour microenvironment and on the lymphoma cell surface. This results in increased B-cell receptor signalling in lymphoma cells and increased production of growth-promoting cytokines by TFH cells, leading to tumour expansion (45, 46).

1.3.3. Advances in the field of molecular diagnostics of lymphomas

New technologies are pushing limits further in the diagnostics of human malignancies, including lymphomas. In the past 20 years advances in the field of next-generation

sequencing (NGS) leading to whole exome and whole genome sequencing studies, development of digital droplet PCR (ddPCR) enabling high-sensitivity molecular studies deepened our knowledge of disease biology. Recently developed methods also opened the field of new sampling methods providing limited nucleic acid input and small tumor fractions like liquid-biopsies and broadened the scope of genetic studies with limited quality tumor tissue samples available like low-coverage whole genome sequencing (lcWGS).

Low-coverage whole genome sequencing is an emerging molecular diagnostic method, enabling high-throughput, robust identification of genome-wide CNAs based on relative depth of coverage (47). This method, utilizing the mapping of single-end sequencing reads to the reference genome and counting those in predetermined genomic windows (called 'bins'), is highly efficient at detecting CNAs from fragmented DNA including circulating cell-free DNA or DNA isolated from formalin-fixed paraffin-embedded tissue samples. Due its cost-effectiveness and high tolerance for input DNA quality, lcWGS is a molecular method with high translational potential. To date, application of the technique in lymphomas has been limited to diffuse large B-cell lymphoma improving the risk prediction for the patients before CAR T-cell therapy (48).

Liquid-biopsy means the analysis of shedding nucleic acids from body fluids surrounding tumor tissues. In lymphomas, analysis of circulating cell-free DNA (cfDNA) in blood plasma led to groundbreaking results in terms of molecular profiling and risk stratification before treatment and response monitoring during treatment and follow-up (49). Analysis of cfDNA has the potential to overcome the difficulties presented by spatial heterogeneity, both in terms of pre-treatment molecular profiling for risk stratification and baseline genotyping for molecular measurable residual disease (MRD) monitoring hence circulating tumor DNA (ctDNA) is shed to the blood stream from all affected disease sites (50). In FL, studies revealed a 31-67% of concordance in shared SNVs between tumor and plasma (51-53). Moreover, several studies showed the value of ctDNA analysis in sensitively monitoring real-time treatment responses in lymphomas (54-57). Although, only few studies investigated the utility of ctDNA analysis in FL for treatment monitoring, a recent study showed, that patients responding to treatment have a more rapid decrease in their ctDNA level (51).

DOI:10.14753/SE.2025.3134

2. OBJECTIVES

During our research we aimed to:

1. Investigate the genetic background of PCFCL including gene mutations of *EZH2* and *TNFRSF14* and assess their association with clinicopathologic parameters, as well as structural genetic alterations
2. Analyze the genome-wide copy number profile of PCFCL using low-coverage whole-genome sequencing
3. Compare the copy number profile of PCFCL to FL to identify biomarkers facilitating differential diagnosis
4. Investigate the association of copy number burden metrics, as well as copy number alterations with clinicopathological parameters in PCFCL
5. Analyze evolutionary trajectories of PCFCL
6. Investigate genetic heterogeneity using paired tumor tissue DNA (tisDNA) and cfDNA samples in R/R FL
7. Analyze the role of spatial heterogeneity in disease evolution in R/R FL
8. Investigate the prognostic role of ctDNA levels in R/R FL

DOI:10.14753/SE.2025.3134

3. METHODS

3.1. INVESTIGATION OF THE GENETIC BACKGROUND OF PCFCL

3.1.1. Patient selection

The study was conducted in accordance with the Declaration of Helsinki and approved by the Ethics Committee of the Hungarian Medical Research Council (45371-2/2016/EKU and IV/5495-3/2021/EKU). All patients gave informed consent for the research use of archival tissue material and clinical data. As both studies were performed using similar methodology, we will discuss them together in the *Methods* part of the thesis, referring to them as *first* and *second* study, where necessary.

We collected and reevaluated 21 cases of PCFCL diagnosed at Semmelweis University, Budapest between 2009 and 2017 for the *first* study and 28 tissue samples from 20 patients diagnosed between 2001 and 2022 at Semmelweis University, Budapest with available representative tumor tissue at diagnosis and/or recurrence for the *second* study. Overall, 8/20 patients were included in both studies. Clinical data was retrieved from the clinical database and reviewed by the care-provider dermatologist. Clinical examinations included thorough physical and routine laboratory examinations (complete blood cell count, serum chemistry studies), chest X-ray, ultrasonography and PET-CT scan. Peripheral blood and occasionally bone marrow involvement was determined by flow cytometry and histological examination. Affected body regions were identified and staging was performed based on the International Society for Cutaneous Lymphomas European Organization for Research and Treatment of Cancer (EORTC) staging guideline for non-mycosis fungoides/Sezary syndrome cutaneous lymphomas (58).

For the *second* study nodal follicular lymphoma (FL) samples were also collected from 64 patients diagnosed between 2002 and 2019 and re-evaluated at Semmelweis University according to the revised 4th edition of World Health Organization criteria (WHO4R) (59).

3.1.3. Histology and immunohistochemistry

Histological analysis of the skin biopsies was performed on formalin-fixed, paraffin-embedded (FFPE) tissues. The histological re-evaluation was performed by two hematopathologists according to the WHO4R classification and EORTC classification (7, 24). The main histological differential diagnosis of PCFCL are reactive follicular hyperplasia, primary cutaneous marginal zone lymphoma (PCMZL), and diffuse large B-

cell lymphoma (DLBCL) with germinal center B cell (GCB) phenotype or leg type. The main pathological findings differentiating PCFCL from reactive lymphoid proliferations were dense, deep dermal, or subcutaneous infiltration of CD20 positive B-cells, clonal expression of IgG light chains, or clonal *IgH* rearrangement; CD10 and BCL6 expressions for the vast majority of the tumor cells together with centrocytic cytology excluded PCMZL; nodularity with expanded presence of FDC network and MUM1 negativity were the main criteria to exclude DLBCL. The LEICA Bond Max fully automatized staining system was used for immunohistochemistry. For antigen localization, DAB polymer (DAKO Denmark) was used. The antibodies employed recognized the following antigens: CD3 (clone QBEnd10), CD20 (clone L-26), Ki67 (clone MIB-1), BCL2 (clone 124), BCL6 (clone PG.B6p), MUM1 (clone M7259), (DAKO, Glostrup, Denmark), CD21 (clone 2G9, Leica, Saint-Petersburg, Russia), and EZH2 (clone 11/EZH2, BD Transduction Lab, San Jose, USA), tonsil samples were utilized as controls. Stained slides were scanned at × 20 magnification using a Panoramic scan instrument (3D Histech, Budapest, Hungary) equipped with a Carl Zeiss objective (NA = 0.83; Carl Zeiss MicroImaging Inc., Jena, Germany). Ki67 expression was quantified with CaseViewer 2.0 (3D Histech, Budapest, Hungary), extended with QuantCenter 2.0 software. The cut off value for BCL2 positivity was 80%, for CD10, BCL6, and MUM1 30%. *IgH* gene rearrangement analysis was carried out for clonality assessment using the BIOMED −2 Concerted Action protocol (60). In the *first* study, EZH2 protein expression was determined in the neoplastic follicles using a semiquantitative method, cases were considered positive if there was moderate to high intensity (2+ or 3+) staining in > 20% of the neoplastic cells. EZH2 positivity was considered high if there were > 50% positive cells in the neoplastic follicles.

3.1.4. Interphase fluorescence in situ hibridization (FISH)

Interphase FISH was performed on 3-μm-thick tissue sections using split signal FISH DNA probe for *BCL2*/18q21 (Vysis LSI BCL2 Dual Color Break Apart rearrangement probe, ABBOTT Molecular diagnostic, Rungis, France) and dual-color probe for 1p36/ 1q25 (Vysis LSI 1p36 SpectrumOrange/Vysis LSI 1q25 SpectrumGreen DualColor Probe, ABBOTT Molecular Diagnostic, Rungis, France) according to the manufacturer's instructions and as described before (61). The FISH signals were visualized using a Nikon Eclipse E600 epifluorescence microscope. Image analysis was performed by using Lucia

Cytogenetics image acquisition system (Laboratory Imaging, Republic of Czech). The cut-off for *BCL2* split positivity and for del 1p36 assessment, lack of one orange (1p36) signal, was set at 20% counting 200 tumor cell nuclei.

3.1.5. Mutation analysis

In the *first* study, DNA was extracted from formalin-fixed paraffin-embedded (FFPE) skin biopsy specimens with tumor tissue presence exceeding 80% using the QIAamp DNA FFPE Tissue Kit (Qiagen) according to the manufacturer's instructions. Bidirectional Sanger sequencing of Y641 (exon 16), A682, and A692 (exon 18) hotspots of the *EZH2* gene and the whole coding sequence of the *TNFRSF14* gene were carried out using custom primers.

3.1.6. Low-coverage whole genome sequencing

In the *second* study, FFPE tissue samples were sectioned for DNA isolation and for the microscopical assessment of tumor cell ratio. In case of low tumor cell purity, tissue blocks were macrodissected to reach a tumor cell content of >50%. DNA was isolated using the QIAamp DNA FFPE Tissue Kit (Qiagen, Hilden, Germany) and quantified using the Qubit HS dsDNA Kit (Thermo Fisher Scientific, Waltham, MA, USA).

Isolated DNA integrity was determined using a multiplex GAPDH PCR approach outlined by van Beers et al. (62) using 2 ng DNA input, 12.5 ul AmpliTaq Gold DNA Polymerase (Thermo Fisher Scientific) and 10 pmol of each primer (Integrated DNA Technologies, Coralville, IA, USA) in a total reaction volume of 25 ul. PCR products were analyzed on a 2.6% agarose gel with GelRed Nucleic Acid Gel Stain (Biotium, Fremont, CA, USA). During library preparation, samples with low integrity (≤2 amplification lines) were amplified with two additional PCR cycles compared to the vendor's recommendation. Formalin fixation induced DNA damages were repaired using the NEBNext FFPE DNA Repair Kit (New England Biolabs, Ipswich, MA, USA). Sequencing libraries were prepared using the NEBNext Ultra II DNA Library Prep Kit for Illumina with NEBNext Unique Dual Index UMI Adaptors (New England Biolabs). After quantification and quality control with the Qubit HS dsDNA Kit (Qiagen) and TapeStation High Sensitivity D5000 Kit (Agilent, Santa Clara, CA, USA), libraries were pooled equimolarly and loaded on a NextSeq2000 (Illumina, San Diego, CA, USA) P2 or P3 flow-cell for 50 cycle, single-read sequencing with a target yield of 10 M bases per library.

3.1.7. Analysis of low-coverage whole genome sequencing data

Raw intensities were converted to raw reads using bcl2fastq (v.2.20.0.422). Raw reads were trimmed using skewer (v.0.2.2) with the mean quality set to 10 and minimum length set to 25 bp in tail mode. Reads were aligned to GRCh38 (downloaded from: https://ftp.1000genomes.ebi.ac.uk/vol1/ftp/technical/reference/GRCh38_reference_genome/) using BWA-MEM (v.0.7.17.) defining read groups and converting aligned reads to the BAM format using SAMtools (v.1.10). BAM files were then sorted by genomic coordinates using GATK SortSam (v.4.1.7) and BAM files from libraries run on a P3 dual-lane flow-cell were merged using samtools merge. Duplicate reads were marked using GATK MarkDuplicates with the optical duplicate pixel distance set to 2500. BAM files processed by GATK ValidateSamFile were analyzed for relative copy number alterations with QDNASeq (v.1.26.0) following standard recommendations in the vignette for normalization and segmentation of coverage data in R (v.4.0.2) using a custom 500 kilobase bin size mappability file available at https://github.com/bataibence/FL-sWGS-heterogeneity/blob/main/QDNAseq_bins_500kb_GRCh38_50bp_mappability_semmelweis.rds. Absolute copy numbers were determined using a custom R script available as a courtesy of George Cresswell. The script performs optimal purity and ploidy search based on creating a fit matrix for every relative alteration in the sample and every purity and ploidy option in order to find a local minima solution. Then, the optimal purity and ploidy solution is used for generating purity and ploidy corrected absolute copy numbers from relative changes. The analysis was performed with ploidy restricted to 2 since hyperdiploid states are rare in follicular lymphoma. Purity search was performed between 0.2 and 1.0 and for samples without a local minima solution, the purity was set to 0.2 in order to detect CNAs. For patients with sequential samples, another analysis run was performed setting purity to 0.1 in order to recover potentially subclonal alterations and alterations in low-purity samples, complemented with an aligned visual inspection of copy number bin profiles.

3.1.8. Analysis of identified copy number alterations and clinicopathological data

Analysis of absolute copy numbers was performed in RStudio Server (v.1.3.959) in R. Absolute copy numbers at or above 3 were considered as amplifications, while absolute copy numbers at or below 1 were considered as deletions. For the determination of

cytoband level and chromosome arm level alterations, we considered only those regions altered, where more than 50% of the respective regions' bases were spanned by bins harboring a deletion or amplification. Distinctive alterations between patient groups were identified using the Fisher's exact test. Visualization of data was performed using the ggplot (v.3.4.2) and ComplexHeatmap (v.2.6.2) packages.

3.1.9. Response criteria and statistical analysis

The association between the different clinicopathological parameters was estimated and compared using the Mann-Whitney U test for continuous variables. Categorical data were compared using Fisher's exact test or MannWhitney statistics. A p value of <0,05 was considered as statistically significant. The Kaplan Meier method was used for the comparison of event free survival (EFS). EFS was defined as time from diagnosis until clinical signs of recurrent disease, administration of anti-lymphoma therapy or death of any cause, whichever occurred first. Time was censored for patients who had not experienced disease relapse or had not died at the time of last follow-up. Statistical analyses were performed using the SPSS 13.0 software and R (v.4.0.2) in RStudio Server (v.1.3.959) in the *first* and *second* study, respectively.

3.2. INVESTIGATION OF SPATIAL GENETIC HETEROGENEITY IN R/R FL ANALYZING CONCURRENT CELL-FREE DNA - TISSUE DNA PAIRS

3.2.1. Patient and sample selection

We investigated 114 samples from 22 relapsed/refractory follicular lymphoma patients who had either paired pretreatment liquid-biopsy and tumor biopsy sample available at the time of disease progression and/or who had available paired tissue biopsies at diagnosis or relapse to determine the level of intrapatient heterogeneity in follicular lymphoma. Altogether we analyzed 62 tumor tissue DNA (tisDNA) samples isolated from FFPE tissue specimens, 29 cell-free DNA (cfDNA) samples isolated from liquid-biopsy samples before or during therapy and 22 genomic DNA (gDNA) samples from peripheral blood mononuclear cells used as germline controls. The patients were diagnosed from 2003 to 2020 in one of five Hungarian oncohematology centers and have been prospectively enrolled in liquid-biopsy collection since 2018.

The study was approved by the Ethics Committee of the Hungarian Medical Research Council (45371-2/2016/EKU and IV/5495-3/2021/EKU) and it was conducted in accordance with the Declaration of Helsinki.

3.2.2. Sample processing and DNA isolation

Liquid-biopsy samples were collected using Cell-Free DNA Collection Tubes (Roche, Switzerland). Blood plasma was isolated using a two-step centrifugation protocol, first centrifuging whole blood at 1600g for 20 min at 4°C, then centrifuging the plasma fraction at 16,000g for 10 min at 4°C. Supernatant was frozen at −20°C and stored at −70°C for a prolonged time until further processing. Cell-free DNA (cfDNA) was isolated using the QIAamp Circulating Nucleic Acid Kit (Qiagen, Germany) following the manufacturer's instructions. Isolated cell-free DNA samples were stored at −20°C.

Tumor DNA was isolated from formalin fixed, paraffin embedded (FFPE) lymph node (LN), bone marrow (BM) and extranodal (EN) lymphoma samples using the QIAamp DNA FFPE Tissue Kit (Qiagen, Germany). Mononuclear cell fraction of peripheral blood samples drawn into EDTA containing blood collection tubes was separated with Ficoll gradient centrifugation (400g for 30 min). Genomic DNA was extracted using the MagCore Plus II Automated Nucleic Acid Extractor (RBC Bioscience Corporation, Taiwan). Quantity of cfDNA, tumor DNA and genomic DNA samples were assessed by a Qubit 4 Fluorometer (Thermo Fisher Scientific, USA). Quality of cfDNA and tumor DNA from FFPE samples were assessed on the 4200 TapeStation System (Agilent Technologies, USA).

3.2.3. Sequencing library preparation

For sequencing library preparation median 105.0 ng (Q1-Q3, 49.7-149.5 ng) cfDNA, median 184.3 ng (Q1-Q3, 148.3-204.5 ng) tumor DNA and median 193.3 ng (Q1-Q3, 186.5-199.6 ng) genomic DNA was used. Tumor DNA and genomic DNA was sheared on the Covaris M220 instrument (Covaris, USA) before library preparation. Library preparation was performed using the SureSelectXT HS Reagent Kit (Agilent, USA), applying the post-capture pooling strategy target-enrichment workflow according to protocol recommendations. For target-enrichment, a custom 1.17 Mb SureSelectXT HS (Agilent, USA) panel was designed covering the whole coding region and UTRs of 173 genes described to be mutated in FL (36, 63-66), as well as regions for *IGH*, *IGL* and *IGK* rearrangement detection and clonotype determination were included. Sequencing

libraries were pooled in equimolar amount and paired-end sequencing was performed on a NovaSeq6000 or NextSeq2000 instrument (Illumina, USA) to a median depth of 6695 (1872-16003) and 2435 (591-3676), respectively.

3.2.4. Pre-processing of sequencing data

Primary analysis of sequencing data was performed to leverage single molecular barcode (MBC) information for read deduplexing to retrieve the highest number of biologically different DNA molecules and to retain read group information to correct for platform and lane specific bias adhering to GATK best practices. Raw intensities were converted to raw reads using bcl2fastq (v2.20.0.422) directing MBC information to a separate FASTQ file for downstream usage. Adaptor sequences were then trimmed with AGeNT (v3.0.6) Trimmer (v.3.0.5) using recommended parameters. Trimmed raw reads were aligned to the UCSC hg19 human reference genome using bwa mem (v0.7.17) and converted to BAM format using samtools (v1.10), followed by sorting and merging of BAM files from different lanes using samtools sort and merge, respectively. Duplicate reads were removed based on MBC information using AGeNT Creak (v1.0.5) in single consensus mode, enabling read filtering based on minimum average MBC base quality (25) and minimum average read base quality (30), as well as enabling consensus read filtering using recommended parameters. Base quality recalibration was performed on duplicate removed BAM files using GATK (v4.1.7.0) BaseRecalibrator using known sites of variation from the 1000G, Mills and 1000G and dbSNP 138 datasets followed by realignment using ApplyBQSR.

3.2.5. Variant calling

Variant discovery was performed using a non-tumor informed pipeline for cfDNA samples in order to retrieve additional variants not detected in tumor DNA. Variants were called and filtered using GATK 4.1.7.0 according to GATK best practices for short variant discovery. Candidate variants were called in tumor DNA and cfDNA samples with GATK Mutect2 using paired genomic DNA as controls. A panel of normals was created from all variants in genomic DNA samples and used for filtering normal artifacts as well as mapping bias. Using LearnReadOrientationModel a read orientation model was built, which can be used to filter both OxoG artifacts, which arise during library preparation and C-T transitions, which are more frequent in FFPE samples due to deamination of cytosine residues during formaline fixation of tissue samples. Then,

potential contamination was calculated using GetPileUpSummaries and CalculateContamination. Finally, variants were hard filtered using FilterMutectCalls considering the contamination and read orientation model created above and optimizing the sensitivity and specificity of the variant filtering process for best precision. Filtered variants were annotated using the Ensembl Variant Effect Predictor (release 106).

Variant call files were then transformed to the MAF format using the vcf2maf tool (v1.6.21) and downstream analysis, visualization and filtering of variants was performed in Maftools (v2.6.05) in R (v4.0.2) using RStudio Server (v1.3.959). In all samples variants were selected with a minor allelic frequency below 0.01% in the gnomAD database (r2.1), considering all samples and harbouring an alternative read count of at least 5, a total read count of at least 50 and a variant allelic frequency above 5% and 0.5% in tisDNA and cfDNA samples, respectively. Variants were further filtered based on either passing all quality filters as per the GATK pipeline or being previously described in the literature and not considered as a normal artifact or contamination. Final variant list was created keeping all variants per patient that met all variant filtering criteria in at least one sample of the patient.

3.2.6. Copy number calling

Copy number alterations were called using the PureCN (v1.20.0) and CNVKit (v0.9.10) packages. PureCN was run separately on the duplicate removed, realigned BAM files sequenced on the NovaSeq6000 and NextSeq2000 platforms with sequencing platform matched genomic DNA controls to account for differences in median sequencing depth. GC correction was performed before copy number calling on all BAM files using the loess method as part of the PureCN workflow. Variant information from Mutect2 calling with the genotype normal and genotype pon sites parameters set to TRUE was used to determine B-allelic frequencies in tumor normal pairs and correct depth of coverage based copy number ratios. Absolute copy number counts were determined after correction for estimated molecular tumor purity and tumor ploidy, with ploidy search restricted between 1.5 and 2.5. CNVKit was run separately on the duplicate removed, realigned BAM files sequenced on the NovaSeq6000 and NextSeq2000 platforms with sequencing platform matched controls. For BAM files sequenced on the NovaSeq6000 platform germline samples were used for copy number calling in FFPE samples, while a negative cfDNA sample was used as control for pretreatment cfDNA samples. For copy number calling

sexes of samples were given as input and molecular tumor purity was used from the PureCN workflow. Absolute copy number counts from PureCN seg files and CNVKit call files were processed to determine position, sub-cytoband and chromosome arm level information. Absolute copy number counts from PureCN call files and CNVKit call files were processed to determine gene level copy number information. When determining sub-cytoband and chromosome arm level copy number alterations only those were considered where the segments harbouring deletions or amplifications were spanning more than 50% of the region. In terms of all resolution levels only those copy number alterations were accepted for downstream processing that were called by both tools with a corrected absolute copy number at or below 1.0 (DEL) or at or above 3.0 (AMP).

3.2.7. Immunoglobulin sequencing and clonotype analysis

Realigned BAM files were analyzed using the WholeMark functionality of ARResT/Interrogate developed for the analysis of *IG/TCR* repertoire using non-amplicon next generation sequencing data as a courtesy of the EuroClonality-NDC Working Group (67). Determined clonotypes were further filtered, visualized and analyzed using R in RStudio.

3.2.8. Phylogenetic reconstruction

Clonal inference was performed on samples of patients with sample triplicates at the same timepoint harbouring at least 5 short variants (PAT-FL-01, -03, -08, -09, and -20, n=15). In order to increase the precision of clonal inference, in addition to non-silent variants in the 173 target genes, variants in *IGH*, *IGK* and *IGL* target regions meeting previously described filters were considered. Variant allelic frequencies before clustering were corrected based on the following parameters: VAFs in positions with a) detected LOH event by PureCN with diploid copy number were divided by 2 b) copy number loss in segment by both tools were divided by 2 c) copy number gain by both tools considering the lower estimated copy number were divided by copy number divided by 2 d) diploid copy number without a predicted LOH event, but with VAF above 50% were divided by 2. Short variants were clustered using SciClone with the maximum cluster number set to 8 and applying default depth filter. Sciclone results were processed in ClonEvol to infer clonal relationship of clusters and create phylogenetic trees. All clonal models were investigated and curated manually to select the most likely model.

3.2.9. Data analysis and statistical methods

The association between the different clinicopathological and genetic parameters was estimated and compared using the Mann-Whitney U test or Kruskal-Wallis test for continuous variables. Categorical data were compared using Fisher's exact test. A p value of <0,05 was considered as statistically significant. The Kaplan Meier method was used for the comparison of progression free survival (PFS). PFS was defined as time from diagnosis until clinical signs of relapse, administration of anti-lymphoma therapy or death of any cause, whichever occurred first. Statistical analyses were performed in RStudio Server in R.

DOI:10.14753/SE.2025.3134

4. RESULTS

4.1. INVESTIGATION OF THE ROLE OF TNFRSF14 AND EZH2 IN THE PATHOGENESIS OF PCFCL

4.1.1. Clinical findings and follow-up

The clinical findings are summarized in Table 1 (68). In our series of 21 patients with PCFCL, the male-to-female ratio was 4:17, with patients being exclusively Caucasian. The median age at diagnosis was 63 years (range 30–82). The clinical presentation was described as erythematous papules, plaques, or nodules. Solitary lesion (stages: T1a, b) was found in 57% of the patients (12/21), multiple lesions were present in 43% (9/21) of the patients (stages: T2a-T3b) especially on the head and neck region (11/21), and on the trunk and upper extremities (8/ 21) or both (2/21). The lower extremities were not involved (Figure 2.). The patients did not have prior diagnosis of lymphoproliferative disease and any associated systemic symptoms (fever, weight loss, or night sweating). No extracutaneous disease, lymph node, or peripheral blood involvement were found at initial and within 6 months of diagnosis. Treatments included surgical excision, radiotherapy or both, and chemotherapy for two patients. Fifteen patients responded initially with complete remission (CR) (Figure 2.), 3 with partial remission (PR).

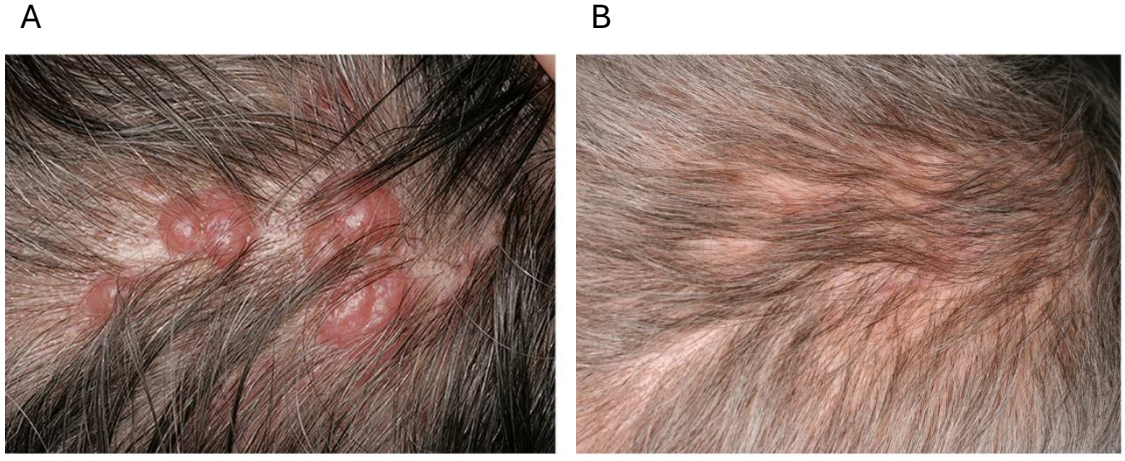

Figure 2. *Clinical picture of a primary cutaneous follicle center lymphoma (PCFCL) with 1p36 deletion (case 1). A) Patient presenting with multiple erythematous papules and nodules on the head. B) Complete remission of the tumor 8 months after diagnosis treated with radiotherapy (68).*

Three patients had multiple lesions at diagnosis and surgical excision was partial. They were followed without any treatment, spontaneous remission occurred in one of them, the other two have stable disease (SD). Relapse occurred in 10 cases, extracutaneous spreading to lymph node was found in one case, who responded with CR after chemotherapy (RCHOP). At the time of the last follow-up, one patient died of pulmonary embolization after 193 months, while in CR, unrelated to the cutaneous lymphoma. All other patients are alive with a median follow-up time of 45 months (7–93), (Table 2.).

Table 2. *Clinical characteristics of the patient cohort (68)*

**Systemic lymph node dissemination detected by PET-CT CR = complete remission, CVP = cyclophosphamide + vincristine + predinisolone, DUD = died of unrelated cause, EFS = event-free survival, F = female, M = male, PCFCL = primary cutaneous follicle center lymphoma, PR = partial remission, R = rituximab, SD = stable disease*

Case	Sex	Age	Stage	Localization	Therapy	Relapse (months)	Disease outcome (follow-up, months)
1	F	75	T2b	Head and neck	Surgical excision + CVP	Yes* (9)	CR (99)
2	F	30	T1a	Head and neck	Surgical excision	Yes (47)	CR (56)
3	F	52	T2a	Head and neck	Radiotherapy	No	CR (14)
4	F	63	T1a	Head and neck	Radiotherapy	No	CR (44)
5	F	67	T1a	Head and neck	Surgical excision	No	CR (55)
6	F	48	T1a	Trunk	Surgical excision	No	CR (47)
7	M	40	T2a	Head and neck	Radiotherapy	No	CR (40)
8	F	68	T2a	Head and neck	Surgical excision	Yes (6)	PR (19)
9	M	42	T1a	Trunk	Surgical excision	Yes (8)	SD (16)
10	F	49	T1a	Trunk	Radiotherapy	Yes (78)	DUD (193)
11	F	66	T2a	Trunk	Radiotherapy	Yes (18)	SD (18)
12	F	63	T1a	Head and neck	Surgical excision	Yes (5)	CR (6)
13	F	56	T2b	Trunk	Surgical excision	Yes (34)	CR (64)
14	F	69	T3a	Head and neck and upper extremities	Observation	No	SD (24)
15	F	68	T2a	Head and neck	Surgical excision	No	SD (7)
16	F	59	T1b	Upper extremities	Surgical excision and radiotherapy	Yes (23)	PR (31)
17	M	70	T1b	Head and neck	Surgical excision	No	PR (14)
18	F	63	T1a	Trunk	Surgical excision and radiotherapy	No	CR (91)
19	F	52	T1a	Trunk	Surgical excision	Yes (33)	SD (68)
20	F	67	T1a	Head and neck	Surgical excision	No	CR (80)
21	M	82	T3b	Head and neck, trunk and upper extremities	R-CVP	No	CR (12)

4.1.2. Histological and immunohistochemical findings

Pure follicular infiltration pattern was observed in most of the cases (17/21). Four cases presented with mixed, follicular/diffuse infiltration pattern. The predominance of small/medium sized centrocytes were seen with few mixed scattered centroblasts in 11/21 cases (grades 1 and 2) while large centrocytes and centroblasts dominated > 50% of the cells (grade 3) in 10/21 cases. Results of the immunohistochemistry are summarized in Table 3.

Table 3. *Results of immunohistochemistry and molecular studies (68)*

**protein expression, 1p36del = 1p36 deletion, IgH = IgH rearrangement*

Case	CD10*	BCL6*	MUM1*	BCL2*	EZH2*	Ki67*	BCL2 split	1p36 del	*TNFRSF14* mutation	*IgH*
1	+	+	-	-	70%	44%	-	+	-	NA
2	+	+	-	+	20%	30%	-	-	-	+
3	+	+	-	+	10%	15%	-	-	-	NA
4	+	+	-	+	50%	43%	-	-	-	+
5	+	+	-	-	60%	44%	-	-	NA	NA
6	+	+	-	-	40%	50%	NA	-	c. 35G>A (p.Trp12*)	NA
7	+	+	-	-	30%	63%	-	-	-	+
8	+	+	-	+	20%	49%	+	-	NA	+
9	+	+	-	-	50%	22%	-	-	NA	+
10	+	-	-	+	0%	1%	-	-	-	NA
11	+	+	-	-	70%	30%	NA	-	-	-
12	+	+	-	+	40%	36%	-	+	-	+
13	+	+	-	-	90%	53%	-	+	-	+
14	+	+	-	+	80%	35%	-	+	c. 157T>G (p.Cys53Gly)	-
15	+	+	-	-	70%	89%	-	+	c. 35G>A (p.Trp12*)	NA
16	+	+	-	+	30%	38%	-	-	-	+
17	+	+	-	-	50%	57%	-	-	-	-
18	+	+	-	-	50%	22%	-	-	-	NA
19	+	+	-	-	50%	10%	-	-	c. 35G>A (p.Trp12*)	NA
20	+	+	-	+	30%	20%	-	-	-	NA
21	+	+	-	+	40%	55%	+	-	NA	+

High proliferation rates above 40% were found in 10/21 cases assessed with Ki67 immunohistochemistry. BCL2 protein expression was observed in 10/21 cases. The BCL2 positive cases tended to have lower proliferation rate than the BCL2 negative ones, but the difference was not significant ($p = 0.198$). BCL6 protein was expressed by the

follicular B-cells in all but one case, in which BCL6 negative tumor cells were positive for CD10. EZH2 protein expression was detected in the neoplastic nodules in all BCL6 positive cases (n = 20) with moderate to high intensity. High EZH2 protein expression (> 50%) was found in 11/21 cases in the neoplastic nodules and was associated with BCL2 negative phenotype (p = 0.009). BCL2 and EZH2 expressions were independent of clinical features and outcome.

4.1.3. Association of the FISH findings with clinical and morphological data

Using FISH, *BCL2* gene break was found in 2/20 cases (10%, Figure 3.), while 1p36 deletion was detected in 5/21 cases (22%, Figure 3.). Cytogenetic abnormalities were strongly associated with stage at diagnosis: more advanced clinical stages with multiple lesions (> T1) were determined at diagnosis in 6/7 (86%) cases with cytogenetic abnormalities compared to cases without *BCL2* gene break or 1p36 deletion (3/14, 21%), (p = 0.016). Other clinical features, including response to therapy and relapse rate did not show any difference between the two groups. Only event-free survival (EFS) showed a tendency to be shorter in the group with cytogenetic abnormalities; however, it did not reach statistical significance (p = 0.052). Ki67 expression tended to be higher in cases with cytogenetic aberrations compared to the negative ones (5/7, 71% vs 5/14, 36%, p = 0.183), with similar BCL2 protein expression in the two groups.

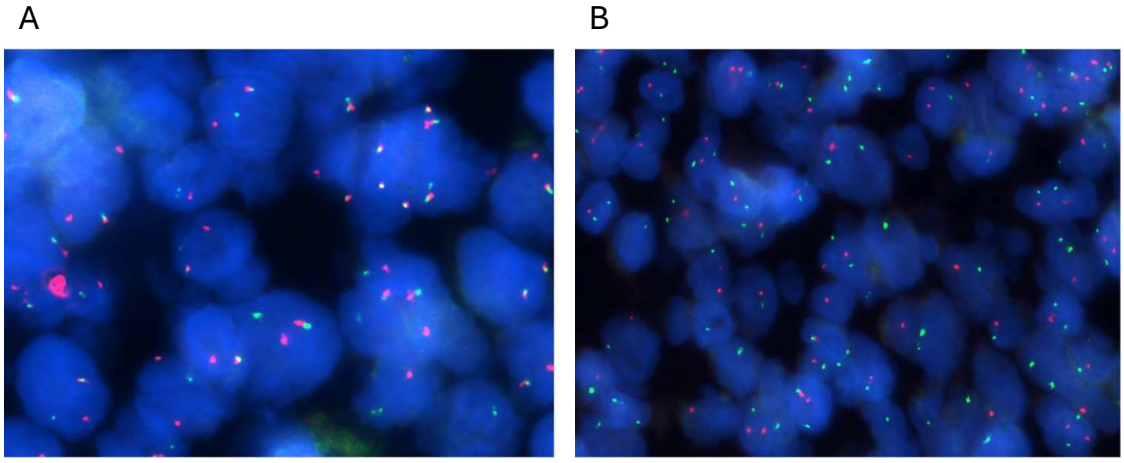

Figure 3. *FISH images of representative cases demonstrating BCL2 break and 1p36 deletion. A) PCFCL showing BCL2 rearrangement using BCL2 Dual Color Break Apart rearrangement probe, with isolated green and red signals. B) PCFCL demonstrating 1p36 deletion using dual-color probe for 1p36/1q25, seen with unique red signals (1p36), whereas two green signals (1q25 control) are observed in tumor cell nuclei (68).*

4.1.4. Mutation analysis and association with clinical data, morphology, and FISH results

We assessed the mutation status of *TNFRSF14* by Sanger sequencing in 17 patients with available DNA samples. *TNFRSF14* mutations were detected in 4/17 (23.5%) patients with three nonsense mutations (c.35G > A; p.Trp12*) previously reported in FL and one previously unreported missense variant (c.157 T > G; p.Cys53Gly) targeting the extracellular domain which is likely to interfere with the ligand binding activity of TNFRSF14 (Figure 4.)(69). Variants previously reported in the dbSNP and 1000 Genomes databases were not considered. Two cases with *TNFRSF14* mutations harbored concomitant 1p36 deletions resulting in complete loss of functional *TNFRSF14*. Significant impact of mutations on clinical features and disease outcome was not observed. Regarding the phenotypic features, 3/4 of the mutant cases were characterized by BCL2 negativity and 3/4 demonstrated high EZH2 protein expression. (Table 3). The presence of gain of function mutations affecting the methyltransferase *EZH2* gene were also assessed at three recurrent mutation hotspots (Y646, A682, and A692), and no mutations were detected in our PCFCL cohort.

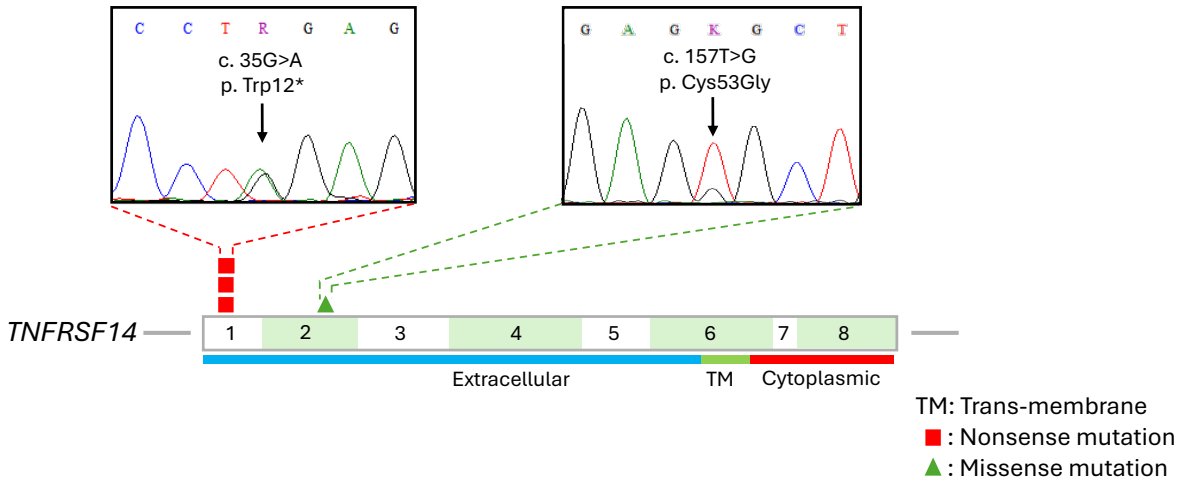

Figure 4. *Mutations identified in TNFRSF14 were exclusively located in the extracellular domain, with three previously reported nonsense mutation and a single case harboring a previously unreported missense variant.*

DOI:10.14753/SE.2025.3134

4.2. ANALYSIS OF COPY NUMBER ALTERATIONS IN PCFCL USING LOW-COVERAGE WGS

4.2.1. Clinicopathological characteristics of the patient cohort

Clinical characteristics of the patient cohort are summarized in Table 4 (70). The male to female ratio was 0.3 and median age at diagnosis was 60 years (range, 35-76 years). Most patients were diagnosed in stage T1a (16/20, 80%), whereas T1b (2/20, 10%) and T2a stages occurred less frequently (2/20, 10%). Clinical presentation was single or multiplex nodules or plaques occurring most commonly on the trunk (9/20, 45%), or on the head and neck (8/20, 40%), while two patients were presenting with lesions on the upper (2/20, 10%) and one on the lower (1/20, 5%) extremities. In addition to surgical excision, radiotherapy was also administered in the first treatment line in eight cases. Median follow-up time and EFS were 61 months (range, 13-157 months) and 23 months (range, 3-83 months), respectively.

Disease recurrence was identified during the disease course in 15/20 patients (75%), affecting the same anatomical region in most of the cases (9/20, 45%), while distant skin recurrences occurred less frequently (5/20, 25%) and systemic spread was observed for only one case (1/20, 5%). The number of recurrences ranged from 1 to 3 (median 2) during the follow-up period.

Pathological characteristics of the 28 analyzed samples from the 20 patients are summarized in Table 5. Altogether, we analyzed 13 samples at primary diagnosis and 15 at recurrence, including sequential samples from 6 patients. Considering all samples, 13/28 (46%) presented with nodular, 12/28 (43%) mixed, and 3/28 (11%) samples with diffuse growth pattern. *IGH::BCL2* translocation status was evaluated by FISH in 15/28 samples and returned a positive result in only one sample (7%). Six out of 21 samples evaluated by FISH for 1p36 deletion were positive (29%).

Using *IGH* sequencing as part of the routine diagnostic workup, 15/28 (54%) samples showed clonal *IGH* rearrangement, 10/28 (36%) showed a non-clonal *IGH* repertoire, while 3/28 (11%) gave no evaluable product.

DOI:10.14753/SE.2025.3134

Table 4. *Clinical characteristics of the patient cohort (70)*

**Stage and region was determined according to the TNM classification system for primary cutaneous lymphomas other than mycosis fungoides and Sézary syndrome*

Patient ID	Sex	Age at diagnosis	Stage at diagnosis*	Region at diagnosis*	First line treatment	Event free survival (mo)	Follow-up (mo)	Recurrence site	Number of recurrences	Samples analysed
Case #1	female	53	T2a	head and neck	surgical excision + radiotherapy	8	13	local	1	primary
Case #2	female	52	T1a	chest	surgical excision + radiotherapy	45	152	distant	3	primary
Case #3	female	66	T1b	upper back	surgical excision + radiotherapy	8	81	local	1	primary
Case #4	female	57	T1a	chest	surgical excision	25	107	local	1	recurrence
Case #5	female	60	T1a	left upper arm	surgical excision + radiotherapy	25	104	distant	3	primary & recurrence
Case #6	female	63	T1a	upper back	surgical excision + radiotherapy	83	83	no		primary
Case #7	female	53	T1a	upper back	surgical excision	3	137	local	2	recurrence
Case #8	female	67	T1a	head and neck	surgical excision	79	79	no		primary
Case #9	female	43	T1a	upper back	surgical excision	63	63	no		primary
Case #10	female	69	T1a	head and neck	surgical excision	34	72	local	1	primary
Case #11	female	68	T1a	chest	surgical excision	14	157	distant	3	2 recurrences
Case #12	female	73	T2a	upper back	surgical excision	32	46	systemic	1	primary & recurrence
Case #13	male	76	T1a	head and neck	surgical excision + radiotherapy	45	45	no		primary
Case #14	male	71	T1b	head and neck	surgical excision	16	34	local	1	recurrence
Case #15	male	64	T1a	head and neck	surgical excision	5	52	local	3	2 recurrences
Case #16	female	57	T1a	left upper leg	surgical excision + radiotherapy	19	43	distant	3	recurrence
Case #17	male	35	T1a	head and neck	surgical excision + radiotherapy	20	20	no		primary
Case #18	male	60	T1a	upper back	surgical excision + radiotherapy	36	57	local	2	2 recurrences
Case #19	female	52	T1a	head and neck	surgical excision	5	27	local	1	primary
Case #20	male	45	T2a	left lower arm	surgical excision	15	59	distant	2	primary & 3 recurrences

Table 5. *Pathological characteristics of patient samples (70)*

(O): another sample of the patient was evaluated

Patient ID	Sample analysed	Region of biopsy	Recurrence site	Systemic treatment before sampling	Elapsed time from diagnosis (mo)	Growth pattern	CD10	BCL2	Ki67	IGH:BCL2 translocation	1p36 deletion FISH	IGH rearrangement
Case #1	primary	head and neck	-	no	0	nodular	+	+	10%	-	-	non-clonal
Case #2	primary	chest	-	no	0	nodular	-	-	50%	-	-	clonal
Case #3	primary	upper back	-	no	0	mixed	-	-	40%	failed	-	non-clonal
Case #4	recurrence	chest	local	no	27	nodular	+	-	80%	-	+	no product
Case #5	primary	left upper arm	-	no	0	mixed	+	-	30%	-	+	non-clonal
Case #5	2nd recurrence	head and neck	distant	no	41	nodular	-	-	15%	- (O)	+ (O)	clonal
Case #6	primary	upper back	-	no	0	nodular	+	-	10%	-	-	clonal
Case #7	1st recurrence	upper back	local	no	30	nodular	-	-	30%	- (O)	- (O)	non-clonal
Case #8	primary	head and neck	-	no	0	mixed	+	+	15%	-	-	clonal
Case #9	primary	upper back	-	no	0	mixed	+	-	25%	failed	-	clonal
Case #10	primary	head and neck	-	no	0	nodular	+	-	5%	- (O)	+ (O)	non-clonal
Case #11	2nd recurrence	head and neck	distant	no	100	mixed	+	+	40%	-	+	clonal
Case #11	3rd recurrence	head and neck	distant	no	106	mixed	+	+	40%	- (O)	+ (O)	clonal
Case #12	primary	upper back	-	no	2	nodular	-	-	40%	-	-	non-clonal
Case #12	1st recurrence	axillary lymph node	systemic	no	39	nodular	+	+	NA	- (O)	- (O)	non-clonal
Case #13	primary	head and neck	-	no	0	mixed	+	-	NA	NA	+	non-clonal
Case #14	1st recurrence	head and neck	local	no	16	diffuse	-	-	80%	-	-	clonal
Case #15	1st recurrence	head and neck	local	no	5	nodular	+	-	20%	- (O)	- (O)	clonal
Case #15	2nd recurrence	head and neck	local	no	12	nodular	+	+	60%	-	-	clonal
Case #16	1st recurrence	left upper leg	local	no	8	mixed	+	+	60%	-	-	clonal
Case #17	primary	head	-	no	0	mixed	+/-	-	30%	-	-	clonal
Case #18	1st recurrence	upper back	local	no	37	nodular	+	+	15%	-	-	clonal
Case #18	2nd recurrence	upper back	local	no	55	nodular	+	+	30%	- (O)	- (O)	clonal
Case #19	primary	head and neck	-	no	0	mixed	+	+	20%	+	-	clonal
Case #20	primary	left lower arm	-	no	0	mixed	-	+	50%	- (O)	-	non-clonal
Case #20	1st recurrence medial	left upper leg	distant	no	16	diffuse	+	+	90%	- (O)	+	no product
Case #20	1st recurrence lateral	left upper leg	distant	no	16	diffuse	+	+	80%	-	+ (O)	no product
Case #20	2nd recurrence	left upper leg	distant	yes	50	mixed	-	+	20%	- (O)	+	non-clonal

4.2.2. Copy number alterations in PCFCL

We performed low-coverage whole genome sequencing on 28 samples of 20 PCFCL patients. At least one CNA was detected in 26/28 (92.9%) samples with median 4 CNAs (IQR: 2-8) per sample. The most frequently identified copy number losses at the cytoband level were the deletions of the 19p12-q13.11 region (28.6%), 1p36.33-p36.23 and 6q24.1 regions (25.0%) as well as the deletions in the 6q16.1-q23.3 regions (21.4%), while the most frequently identified copy number gains were spanning the 2p22.2-p15 (32.1%), 2p22.3 (28.6%), 12q13.13-q14.3 (25.0%) and 1q21.2-q25.3 (25.0%) regions (Figure 5.) Arm level deletions were most frequently affecting the 6q, 19p and 19q chromosome arms (all, 10.7%), while arm level amplifications were present in the 1q, 7p and 7q chromosome arms in 21.4% of all samples. Amplifications were more often conferred by arm level changes, while deletions were often focal. Focal amplification was detected in 59 of 508 (11.6%) altered cytobands while focal deletion was observed in 126 of 273 (46.2%) altered cytobands.

Deletions of 1p36 were investigated by both FISH and lcWGS in 20 samples (Figure 5.). Out of these, 13 samples provided a concordant negative result, while 4 samples had a concordant positive result. In 2 samples, only FISH was positive, while in 1 sample a 1p36 deletion was solely identified using lcWGS. Overall, this resulted in a positive and negative predictive value of lcWGS for the 1p36 deletion of 80% and 87%, respectively. Clonality assessment was successfully performed in 25/28 samples using *IGH* sequencing. Notably, in all 3 samples with no product during clonality analysis multiple CNAs could be detected providing clear evidence of clonal proliferation. Furthermore, in all samples with a non-clonal *IGH* repertoire (n=10), one (3/10, 30%) or multiple (7/10, 70%) CNAs were identified (Figure 5.).

4.2.3. Comparison of the copy number profiles of PCFCL and nodal follicular lymphoma

Subsequently, we compared the copy number profiles of PCFCL samples to data generated from a process-matched cohort of diagnostic, pre-treatment nodal follicular lymphoma (FL) samples (n=64), constituting of patients with limited stage disease (Ann Arbor I-II) in 13.5% and advanced stage disease (Ann Arbor III-IV) in 86.5% of cases. To remove the distortion effect of sequential samples in the PCFCL cohort, we performed

DOI:10.14753/SE.2025.3134

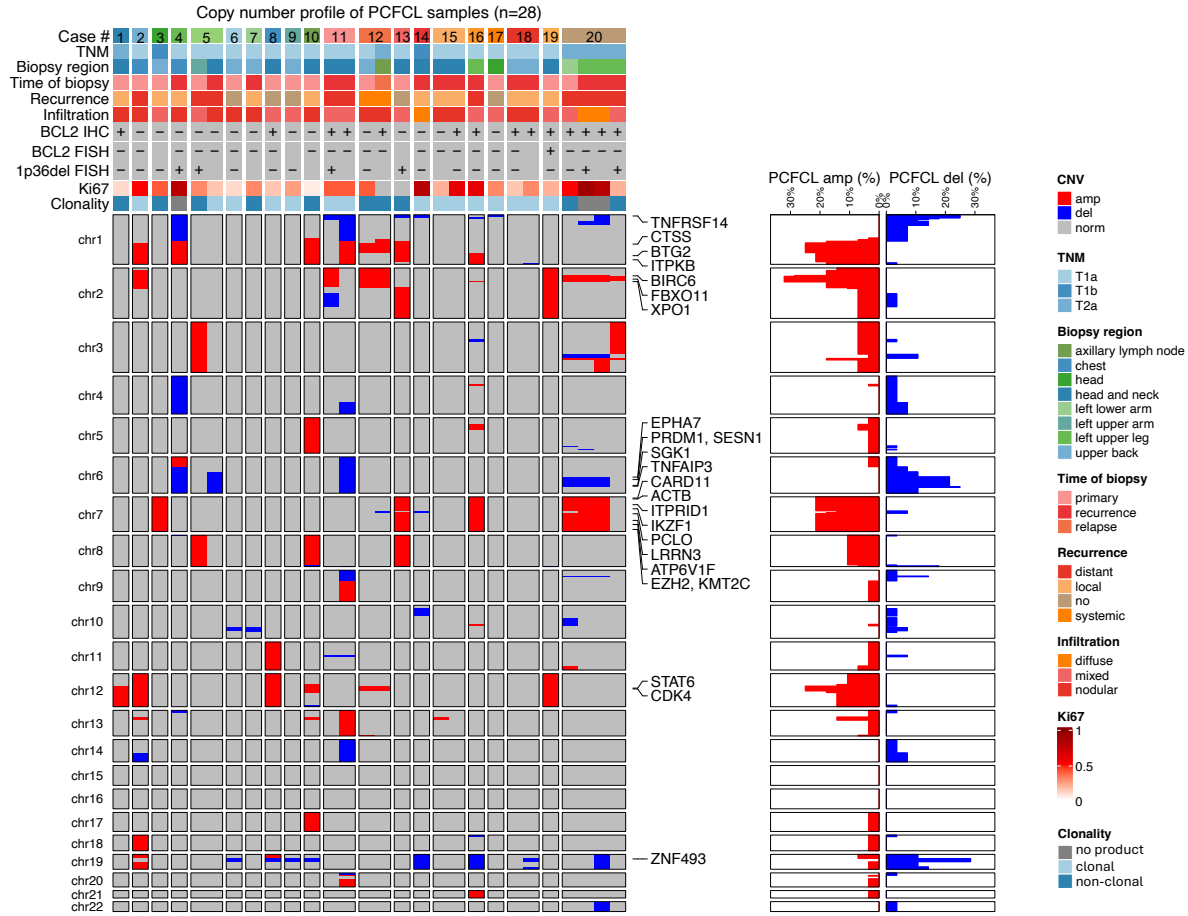

Figure 5. *Copy number profile of all primary cutaneous follicle center lymphoma (PCFCL) samples analyzed in the study (n = 28) displaying associated clinicopathological characteristics and frequency of copy number alterations (CNA). Genes in regions harboring a copy number alteration in at least 20% of the samples are displayed on the right side of the heatmap (70).*

Abbreviations: amp: amplification, del: deletion, FISH: fluorescence in situ hybridization, IHC: immunohistochemistry, norm: normal, TNM: tumor, node, metastasis stage of cutaneous lymphomas other than mycosis fungoides and Sezary syndrome.

the analysis including only on the first sample of each patient. Investigating copy number burden metrics, the median proportion of genome altered (PCFCL: 0.06, IQR: 0.01-0.14 vs. FL: 0.07, IQR: 0.04-0.14, p=0.400, Wilcoxon test), as well as the median number of identified copy number changes were similar between the two patient groups (PCFCL: 4, IQR: 2-8 vs. FL: 4, IQR: 2-7, p=0.370, Wilcoxon test)(Figure 6.).

DOI:10.14753/SE.2025.3134

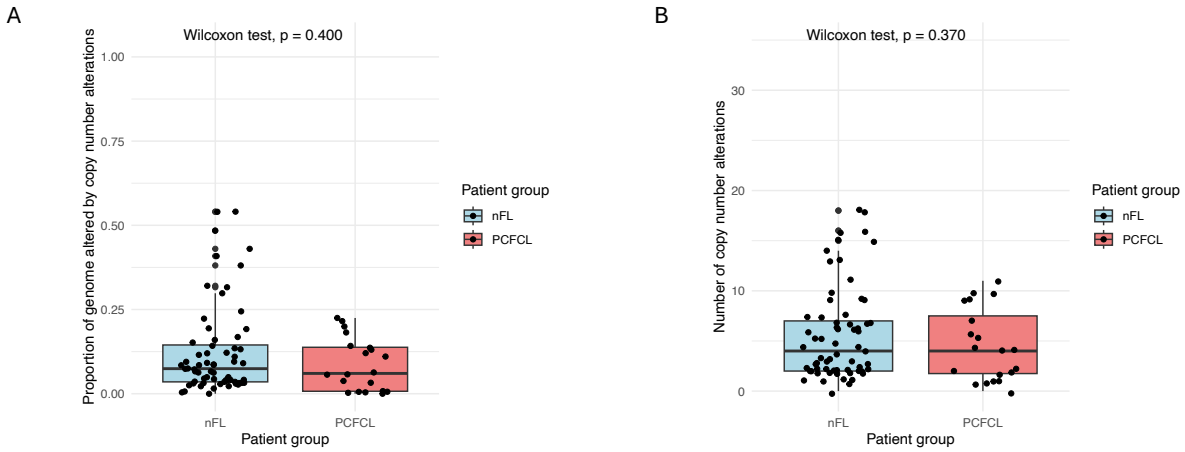

Figure 6. *Comparison of copy number burden metrics and frequency of distinctive copy number alterations between nodal follicular lymphoma (FL, n=64) and primary cutaneous follicle center lymphoma (PCFCL, n=20) samples including the first sample of every patient. A) Comparison of proportion of genome altered by copy number changes between FL and PCFCL. B) Comparison of the number of identified copy number changes between FL and PCFCL (70).*

Our results indicated relatively similar copy number profiles of PCFCL and FL (Figure 7.). Most frequent CNAs in both cohorts were deletions on 1p and 19p chromosome arms affecting *TNFRSF14* and *ZNF493*, respectively, and amplifications on 1q, 2p and 12p chromosome arms spanning the coding regions of *CTSS*, *BIRC6*, *FBXO11*, *XPO1*, *STAT6* and *CDK4*.

Interestingly, out of the most frequent alterations known in FL, amplifications on chromosome 18q peaking at the 18q21.33 cytoband and affecting the locus of the *BCL2* oncogene showed significant enrichment in FL samples (31.3% (20/64), while it was detected only in one PCFCL sample (5.0% (1/20), p=0.018, Fisher's exact test) (**Figure 7**). Significant enrichment of amplifications in the 13q14.11-q14.2 region was observed in PCFCL (PCFCL: 15.0% (3/20) vs. FL: 1,6% (1/64), p=0.040, Fisher's exact test) spanning the coding region of *FOXO1*. After including all PCFCL samples in the analysis to account for potential temporal heterogeneity, all identified distinctive regions remained significantly enriched in either subgroup. Additionally, the absence of deletions in the 10q23.32 cytoband was observed as a distinctive feature between PCFCL and FL samples (PCFCL: 0.0% (0/28) vs. FL: 17.2% (11/64), p=0.017, Fisher's exact test).

DOI:10.14753/SE.2025.3134

Despite the low prevalence of *IGH::BCL2* translocation and 18q21.33 amplification commonly leading to BCL2 overexpression in FL, BCL2 expression was still observed in 50% (14/28) of PCFCL samples by immunohistochemistry using a conservative BCL2 cut-off above 80%, with further three cases harbouring a BCL2 expression between 50-80% considered as negatives. Scrutinizing the differences between the CNA profiles of PCFCL samples showing BCL2 positive vs negative phenotypes, we did not observe significantly enriched alterations in BCL2 positive cases. Interestingly, 2p22.2-p15 amplifications encompassing the *XPO1* and *REL* genes, potentially enhancing the BCL2 expression via the NF-kB pathway, were detected in more BCL2 positive samples, although this difference was not statistically significant (14.3% (2/14) vs. 50.0% (7/14), p=0.103).

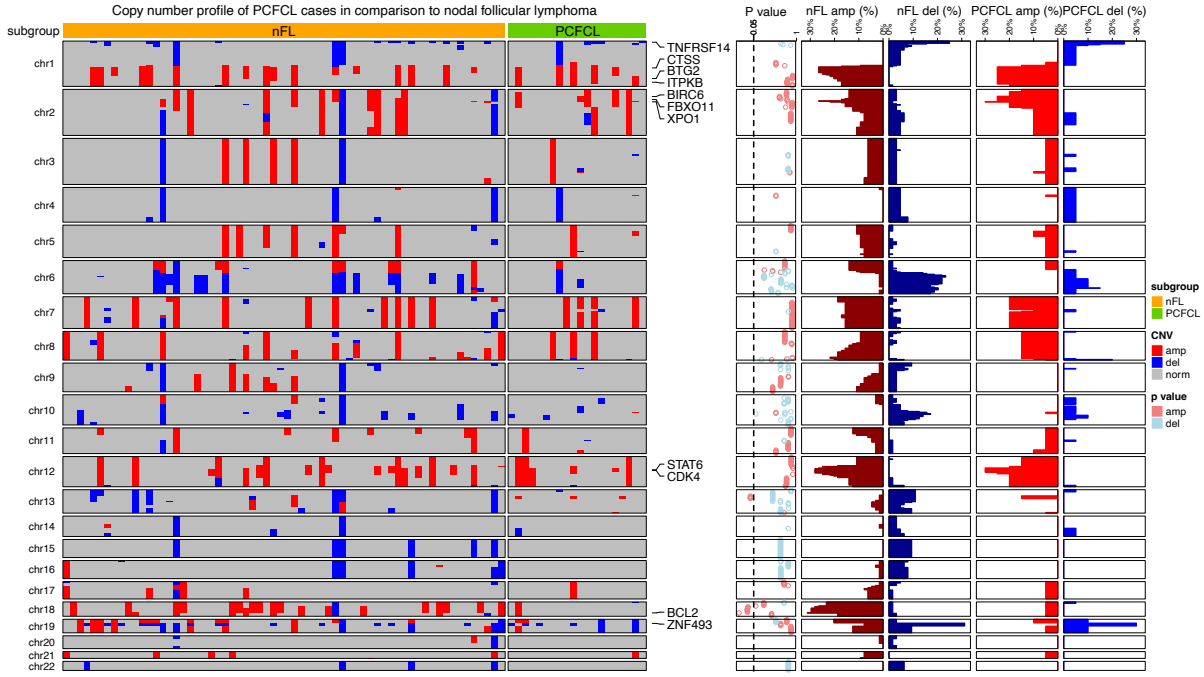

Figure 7. *Copy number profile of primary cutaneous follicle center lymphoma (PCFCL) cases in comparison to a cohort of process-matched nodal follicular lymphoma (FL) samples. The heatmap displays the copy number profile of FL (n=64) and PCFCL (n=20) samples, highlighting the most frequently affected (frequency above 25% in any of the cohorts) genes on the right side of the heatmap. P values of the Fisher's exact test for the corresponding cytoband are displayed on the dotplot on the right side of the heatmap for values below 1.0. Next to the p values, the frequency of deletions (del) and amplifications (amp) are visualized separately for each group as barplots (70).*

4.2.4. Prognostic significance of copy number alterations in PCFCL

To identify CNAs potentially associated with disease recurrence, we investigated the differences between the copy number profiles of unrelated primary and recurrence samples. Median proportion of genome altered (primary: 0.11 (IQR: 0.03-0.14) vs. recurrence: 0.04 (IQR: 0.01-0.10), p=0.490) and the number of CNAs (primary: 4 (IQR: 2-7) vs. recurrence: 4 (IQR: 2-8), p=1.000) showed no difference between the patient groups. Investigating potentially distinctive regions, significant enrichment of 1p36.23-p36.22 deletions were found in the recurrence samples spanning the coding region of *MTOR* (7.7% (1/13) vs. 57.1% (4/7), p=0.031).

Stratifying patients by distant cutaneous recurrence, omitting the case developing systemic propagation from the analysis proportion of genome altered (localized: 0.04 (IQR: 0.01-0.13) vs. distant: 0.13 (IQR: 0.12-0.14), p=0.190) and number of CNAs (localized: 2 (IQR: 1-6) vs. distant: 10 (IQR: 4-10), p=0.044) were moderately higher in patients developing distant cutaneous spread. Amplifications on the 2p arm were significantly enriched peaking in the 2p15 cytoband coding *XPO1* (7.1% (1/14) vs. 80.0% (4/5), p=0.006) and in the neighbor 2p22.3-p16.1 cytobands coding *REL* (7.1% (1/14) vs. 60.0% (3/5), p=0.037).

Analyzing all PCFCL samples, copy number burden was significantly higher in samples of patients' developing distant cutaneous spread both in terms of proportion of genome altered (localized: 0.02 (IQR: 0.01-0.12) vs. distant: 0.13 (IQR: 0.07-0.16), p=0.033) and number of CNAs (localized: 2 (IQR: 1-5) vs. distant: 9 (3-11), p=0.017) pointing to higher genomic instability in samples more readily involving distant disease sites (Figure 8.). Additionally, the enrichment of 12q amplifications was also observed in primary samples peaking in the 12q13.13-q14.3 region coding *STAT6* and *CDK4* (46.2% (6/13) vs. 6.7% (1/15), p=0.029), while 3q23-q24 amplifications (0.0% (0/16) vs. 41.7% (5/12), p=0.008) and 9p21.3 deletions (0.0% (0/16) vs. 40.0% (4/10), p=0.014 covering *CDKN2A* and *CDKN2B* in addition to deletions of 6q16.1-q23.3 (6.3% (1/16) vs. 50.0% (5/10), p=0.018) covering *PRDM1* and *TNFAIP3* were more frequently observed in patients developing distant cutaneous spread (Figure 8.). We analyzed the prognostic significance of recurrent copy number alterations using the Kaplan-Meier method, yet EFS was not associated with alterations in any of the investigated cytobands based on the log-rank test.

DOI:10.14753/SE.2025.3134

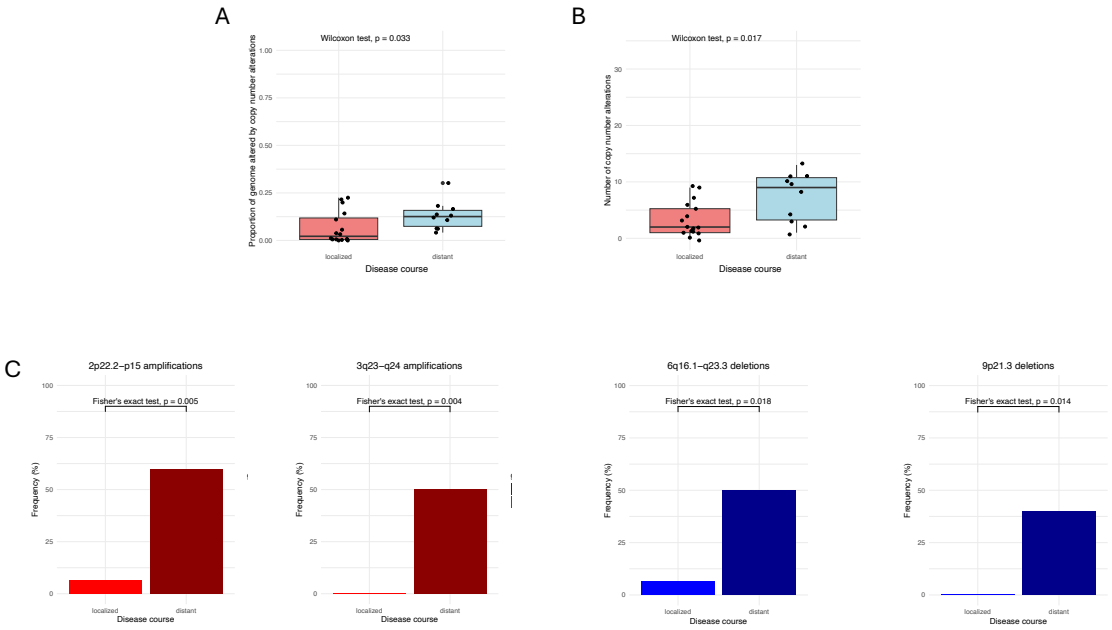

Figure 8. *Distribution of copy number burden metrics and alterations in distinctive regions between primary cutaneous follicle center lymphoma (PCFCL) patients showing localized disease course compared to patients developing distant cutaneous spread or systemic disease. A-B) Proportion of genome altered and the number of identified copy number alterations were significantly higher in patients with distant disease spread suggesting increased genomic instability. C) Including all samples, 2p22.2-p15 and 3q23-q24 amplifications, as well as 6q16.1-q23.3 and 9p21.3 deletions were detected as potentially prognostic biomarkers of the disease course in PCFCL (70).*

4.2.5. Evolution of the copy number profile of PCFCL during the clinical course

Comparing the copy number profiles of sequential tissue samples from 6 patients, overlapping alterations were observed in 3 patients during the disease course with additional emerging and diminishing alterations underlining the role of spatiotemporal heterogeneity in the pathogenesis of PCFCL (Figure 5.). In two patients, there were no copy number alterations in one of the samples potentially pointing to a flat copy number profile. In case #5, the primary and recurrence sample harbored different alterations, including chromosome 3 and 8 amplifications and 1p36 deletion in the primary sample, but an isolated 6q deletion in the recurrence sample (Figure 5.). Additionally, the primary and recurrence samples showed marked differences in phenotype and *IGH* repertoire usage. The primary sample showed mixed nodular and diffuse proliferation with BCL6,

CD10 and BCL2 positivity and a polyclonal *IGH* profile, while the recurrence sample showed nodular, BCL6 positive, CD10 and BCL2 negative, *IGH* monoclonal proliferation, suggesting the parallel development of two separate malignant clones, with the second one expanding at recurrence.

With regard to the clinical outcome, two patients with available sequential samples displayed an unfavorable clinical course, one with development of systemic spread (case #12), or distant skin recurrence and underlying soft tissue infiltration requiring chemoimmunotherapy (case #20).

Case #12 had a history of erythematous plaques on her back for 3.5 years, when surgical excision of a plaque and a cutaneous nodule was performed. Histology revealed PCFCL with nodular growth pattern, with CD10, BCL2 negative centrocytic infiltrate (Figure 9.). Staging found no evidence of systemic involvement. Thirty-seven months later, multiplex enlarged lymph nodes were detected in the right axillary region. Pathological examination of the core biopsy revealed infiltration of CD10 and BCL2 positive nodular centrocytic infiltration consistent with classical follicular lymphoma (Figure 9).

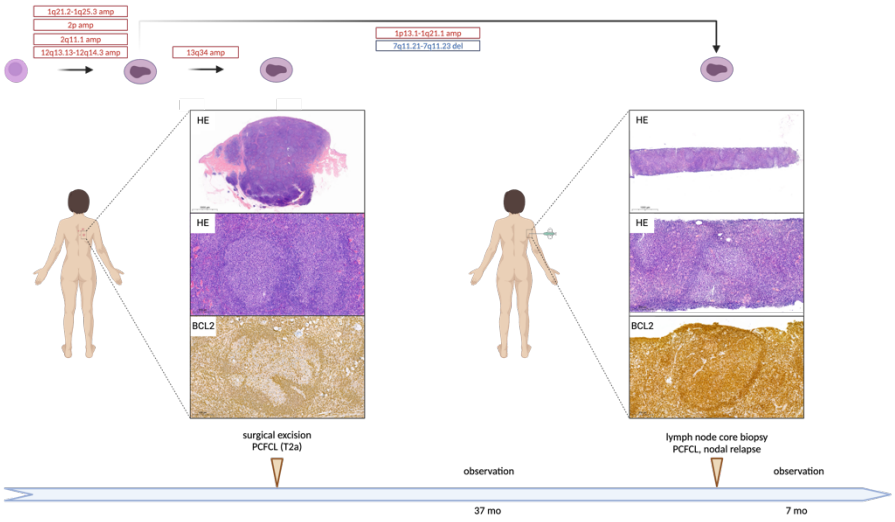

Figure 9. *Comprehensive overview of disease course in case #12 developing systemic propagation to secondary nodal follicular lymphoma (FL). Case #12 was diagnosed with stage T2a PCFCL at the age of 73, which harbored a 1q21.2-q25.3, 2p arm, 2q11.1, 12q13.13-q14.3 and 13q34 amplification as later revealed by low-coverage whole genome sequencing. After 32 months of observation, right axillary lymphadenopathy was detected. Low-coverage whole genome sequencing uncovered the previously identified amplifications in the background of systemic propagation except for the 13q34*

amplification with newly acquired alterations such as a 1p13-q21.1 amplification and a 7q11.21-q11.23 deletion (70).

Spontaneous regression of the lymph nodes was observed on ultrasonography during the watch and wait period and the patient does not have any lymphoma related symptoms at the end of follow up. In the primary sample lcWGS recovered amplifications in the 1q21.2-q25.3, 2p arm, 2q11.1, 12q13.13-q14.3 and 13q34 regions. The previously identified amplifications were uncovered in the lymph node sample except for the 13q34 amplification with newly acquired alterations including a 1p13-q21.1 amplification and a 7q11.21-q11.23 deletion (Figure 9.).

Case #20 presented with a subcutaneous nodule on his lower left arm, accompanied by erythematous papules on his left upper arm, showing mixed nodular and diffuse infiltration of centrocytes consistent with PCFCL (Figure 10.). Sixteen months later, the disease recurred as a fast-growing subcutaneous nodule in the medial part of the left thigh surrounded by a group of small papules, as well as erythematous plaques on the lateral side of the hip. Histological examination of the medial nodule revealed subcutaneous diffuse infiltration of mostly centroblasts accompanied by high number of mitotic and apoptotic figures, while the lateral lesion showed monotonous, diffuse, large centrocytic infiltrate with blastoid morphology in the dermis. Leg-type DLBCL was excluded in both cases based on MUM1 negativity and lack of immunoblasts, the presence of centrocytes, and negative results for *BCL2*, *BCL6* and *MYC* translocations by FISH. PET-CT restaging described increased subcutaneous and deep soft tissue 18-fluorodeoxyglucose uptake near the lesions with no evidence of further systemic involvement. Suspected soft tissue involvement indicated chemoimmunotherapy treatment resulting in complete morphometabolic remission. Thirty-four months later a relapse occurred in the left thigh and around both ankles. Surgical excision from the left thigh revealed nodular centrocytic infiltrate with BCL6, BCL2 co-expression and low proliferation rate, consistent with classic PCFCL resembling the primary sample. Since the surgical excision the patient has been in complete remission.

DOI:10.14753/SE.2025.3134

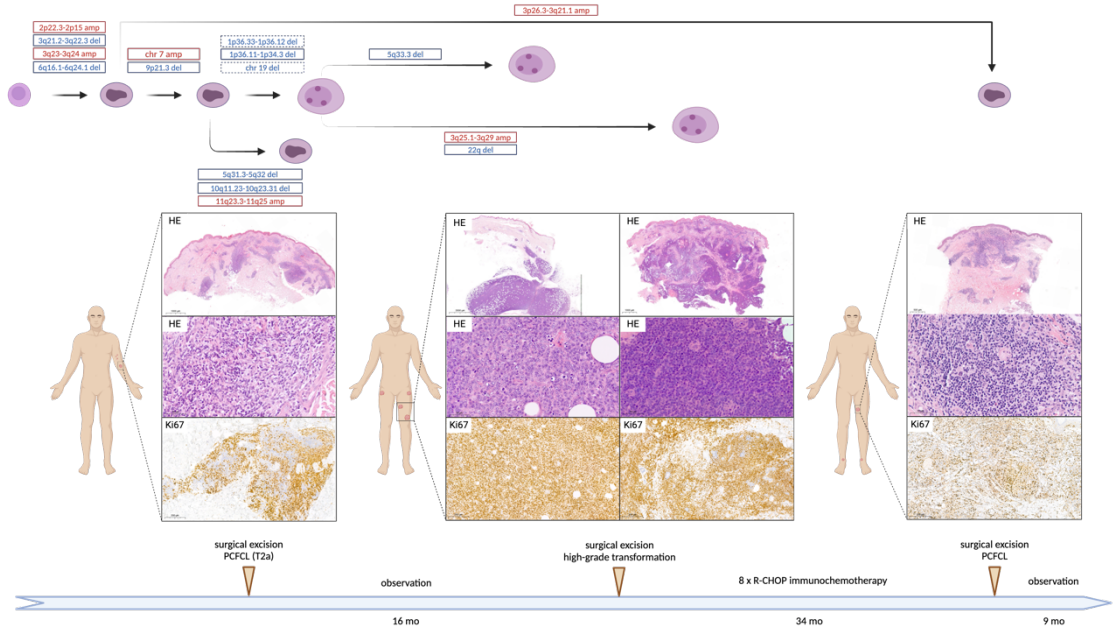

Figure 10. *Comprehensive overview of disease course in case #20 developing high-grade recurrence requiring chemoimmunotherapy. Low-coverage whole genome sequencing revealed 2p22.3-p15 and 3q23-q24 amplifications, as well as 3q21-q22.3 and 6q16-q24.1 deletions in all four samples of the patient possibly representing the earliest events in lymphomagenesis, with the clone later acquiring lymphoma specific alterations such as 1p36 deletion potentially facilitating clinical and morphological progression. Systemic chemoimmunotherapy successfully eliminated the expanded highly proliferating subclone, but the disease resembling the earliest common precursor recurred as a low-grade process (70).*

In the respective primary sample, lcWGS revealed 2p22.3-p15 and 3q23-q24 amplifications, as well as 3q21-q22.3 and 6q16-q24.1 deletions that were detected throughout the clinical course, in addition to chromosome 7 amplification and 9p21.3 deletion common to the clone leading to high-grade relapse, morphologically resembling the systemic high-grade B-cell lymphoma diagnostic category. Amplification of 11q23.3-q25 and 5q31.3-q32, as well as deletion of 10q11.23-q23.31 was specific to the primary sample (Figure 10.). At first relapse, both morphologically high-grade tumor samples acquired a 1p36.33-p36.12 deletion and a chromosome 19 deletion, albeit these were subclonally detected in the medial lesion, and a 1p36.12-p34.3 deletion that was observed clonally in both samples. Furthermore, in the medial lesion a 5q33.3 deleted subclone,

while in the lateral lesion a 3q25.1-q29 amplified and 22q deleted subclone expanded, pointing to spatially separated evolution. Systemic chemoimmunotherapy successfully eliminated the expanded high-grade subclone, but the disease recurred resembling the earliest common precursor with predominantly small centrocytic infiltration harboring an additional 3p26.3-q21.1 amplification (Figure 10.).

4.3. INVESTIGATION OF SPATIAL GENETIC HETEROGENEITY IN R/R FL ANALYZING CONCURRENT CELL-FREE DNA – TISSUE DNA PAIRS

4.3.1. Clinical characteristics of the patient cohort

Molecular profiling of recurrently mutated genes, copy number alterations and immunoglobulin gene rearrangements were performed on 91 tisDNA or cfDNA samples of 22 R/R FL patients (71). Median age at diagnosis was 58 years, with a male to female ratio of 1.75. Most patients were diagnosed with advanced stage disease (Ann Arbor III-IV, 17/20), while 3/20 patients were diagnosed with limited stage FL (Ann Arbor I-II). 18/22 patients received upfront treatment with immunochemotherapy (16/22), radiotherapy (1/22) or chemotherapy (1/22), while 4 patients were started on a watch and wait approach. 14/18 patients responded to first line anti-lymphoma treatment, yet progression of disease within 24 months from start of first line therapy (POD24) was observed in 9/22 patients. Initial disease presentation was localized to lymph nodes (21/22) and showed low grade morphology (17/22) in the majority of the cases, with only one case of composite FL-DLBCL. Median progression free survival in first line was 3.29 years, with patients requiring median 3 treatment lines (range, 1-6) during the follow-up. Pre-treatment liquid-biopsy sampling was performed before any systemic treatment in 4/24, after one line in 8/24, after two lines in 9/24, after three and four treatment lines in 2/24 and 1/24 samples, respectively. In the subsequent treatment line after cfDNA sampling patients harboured more features associated with high-risk disease including a shift towards higher FLIPI scores compared to baseline (low: 3/22, intermediate: 3/22, high: 16/22). At this time, patients received immunochemotherapy or combined immunotherapy in the case of 23/24 samples and responded with shorter, median 1.36 years progression free survival.

4.3.2. Overview of the mutation profile

Non-silent single nucleotide variants and small indels were identified in 21 of 24 (87.5%) pretreatment cfDNA samples. In positive cfDNA samples median 7 variants (range: 1-34) were identified in 75 out of 173 genes in the sequencing panel previously shown to harbor mutations in FL. Considering 20 patients who had a pretreatment cfDNA sample at relapse 18/20 patients (90.0%) harbored at least one detectable alteration at relapse with three patients harboring mutant cfDNA samples before two treatment lines during the disease course.

Non-silent small variants were detected in 59 of 62 tumor tissue samples, with median 9 variants per sample (range: 1-32). Two out of three tissue samples without a detectable alteration were bone marrow samples with visible follicular lymphoma infiltration of less than 10 percent of all cells.

Considering all samples, the most frequent alterations were *KMT2D* (65%), *CREBBP* (54%), *TNFRSF14* (41%), *EZH2* (24%) and *EP300* (20%) mutations (Figure 11.). Cytosine to thymine transitions were the most frequent events both in cfDNA and tisDNA samples, with missense variants dominating the mutation landscape (61.7%, 523/847 variants).

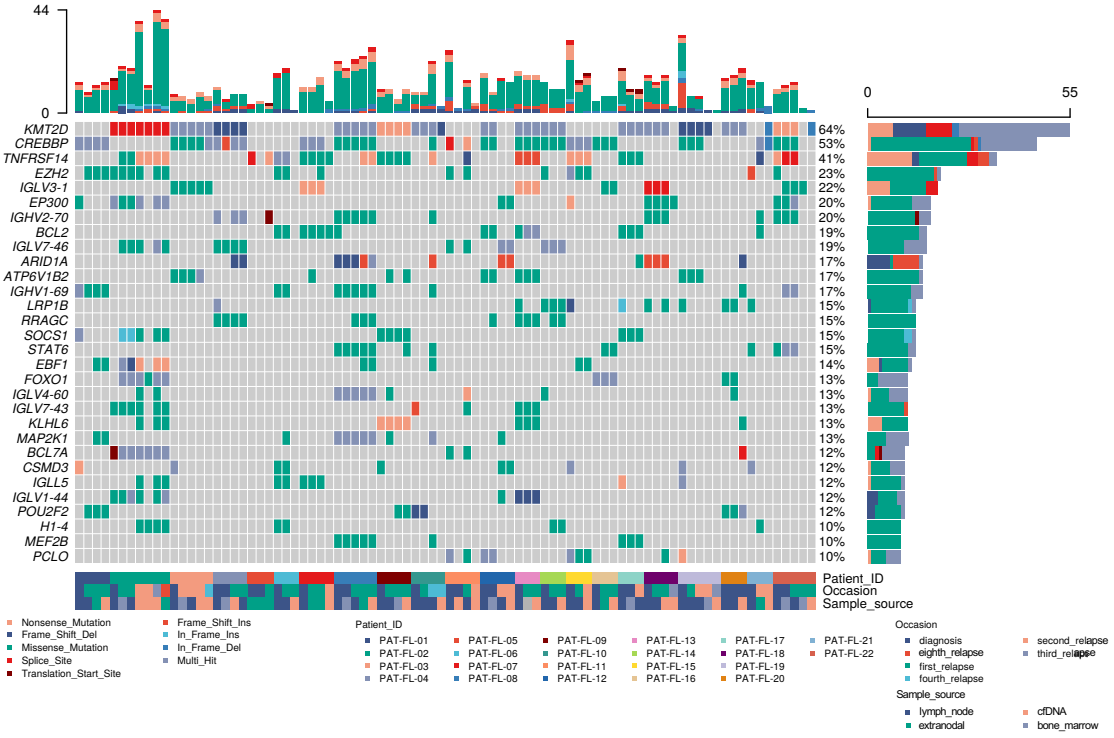

Figure 11. *Oncoplot of identified variants in all samples using tumor-informed filtering*

4.3.3. Spatial genetic heterogeneity between FL compartments

Focusing on the genetic heterogeneity between pretreatment cfDNA samples and concurrent tumor tissue samples before the same treatment line, we compared variants in 20 tumor tissue samples of 15 patients to corresponding cfDNA samples. As variant filtering metrics are known to influence variant recovery, at first we compared multiple filtering methods (Figure 12.). Retaining both silent and non-silent variants using a tumor-naïve approach resulted in the lowest median overlap (37.5%, IQR: 3.6%-69.8%), which increased to 41.4% (IQR: 9.0%-72.7%), when we only considered non-silent variants. Performing tumor-informed filtering, retaining called variants in all samples meeting filtering quality metrics in at least one of the patient samples increased variant overlap to median 63.6% (IQR: 28.2%-86.2%), which could be only modestly increased when we restricted the variant discovery list to positions sequenced to a unique molecule depth of 1000x in all patient samples (69.0%, IQR: 34.8%-84.4%).

Furthermore, using tumor informed filtering more unique variants were recovered in cfDNA (14.8%, IQR: 0.0%-33.1%) than tisDNA samples (9.8%, IQR: 0.0%-24.7%).

Investigating spatial heterogeneity in tisDNA-cfDNA sample pairs, there were 4 sample pairs in which there was complete overlap considering variants, while in two pairs there was no detectable alteration in cfDNA samples (Figure 12). The additional 15 sample pairs showed marked heterogeneity regarding cfDNA and tumor biopsy comparison with the frequency of overlapping variants ranging from 4.55% to 83.33%. Variants were only detected in the cfDNA compartment in 4.55% to 88.24% of total variants per sample. When comparing spatial compartmentalization of variants to tisDNA pairs from concomitant nodal, or extranodal-nodal pairs in 5 patients, we found that concordance of variants was comparable to cfDNA-tisDNA pairs (62.5%, IQR: 53.8%-72.9%)(Figure 12.), but higher than tisDNA pairs from concomitant nodal/extranodal and histologically infiltrated bone marrow biopsies (44.4%, IQR: 36.4%-66.7%) (Figure 12).

4.3.4. Spatial dynamics of subclones in FL

Clonal inference was performed in patients harbouring sample triplicates including 2 tisDNA and a cfDNA from the same timepoint. Variants in immunoglobulin genes were also involved in the analysis in order to increase the number of variants leading to more precise clustering. Altogether the 15 samples harboured 208 non-silent variants localized

DOI:10.14753/SE.2025.3134

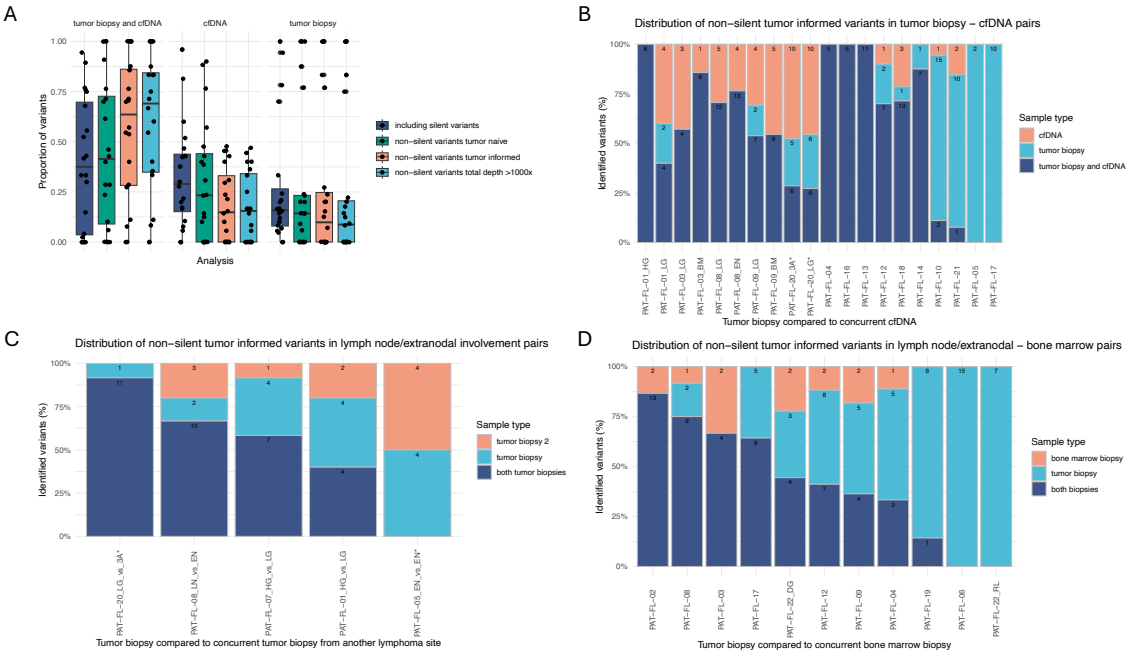

Figure 12. *Spatial distribution of variants across compartments using tisDNA-tisDNA and tisDNA-cfDNA sample pairs. A) Spatial distribution of variants between cfDNA and tisDNA using different variant filtering methods. B) Spatial distribution of non-silent tumor informed variants between cfDNA-tisDNA compartments C) Spatial distribution of non-silent tumor informed variants between tisDNA-tisDNA compartments including lymph node-lymph node, lymph node-extranodal and extranodal-extranodal sample pairs. D) Spatial distribution of non-silent tumor informed variants between lymph node-bone marrow or extranodal involvement-bone marrow sample pairs.*

to 90 unique variant positions with median 12 variants per sample (range, 6-28).

Investigating spatial dynamics of subclones based on variant clustering revealed two patterns contributing to spatial heterogeneity. In 4/5 patients a subclone was spatially restricted, meaning that it was only recoverable in one of the tisDNA samples, but readily recovered in the cfDNA compartment (Figure 13.). Additionally, this spatially restricted subclone was shown to harbor the capability of driving disease progression, as evidenced in case #1, where the spatially restricted subclone characteristic of the transformed duodenal mass was harboring a *MAP2K1, EBF1, EZH2* and *BTK* mutation including genes known to be potent drivers of high-grade transformation. Interestingly, in 3/5 patients an occult subclone was also detected, that was only recovered in the cfDNA

DOI:10.14753/SE.2025.3134

compartment, but detected in none of tisDNA samples (Figure 13.). Additionally, in case #3 it was shown, that the cfDNA and bone marrow tisDNA samples were able to capture more accurately the clonal composition of the relapse sample two treatment lines later than the nodal tisDNA.

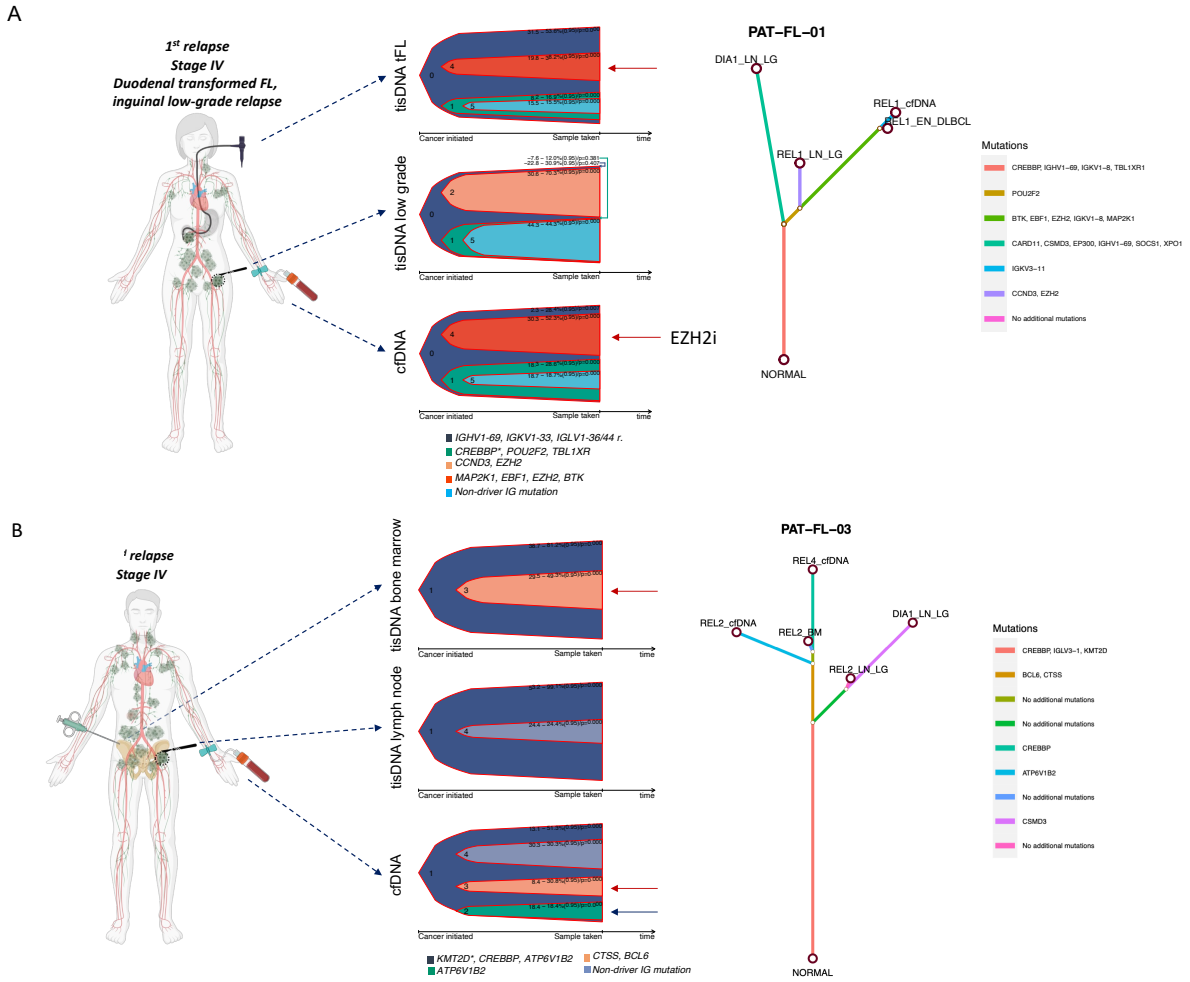

Figure 13. *Spatial dynamics of subclones in FL. A) A representative case showing a spatially restricted subclone potentially driving disease progression through the selection of MAP2K1, EBF1, EZH2 and BTK mutations in the transformed duodenal mass readily recovered in the cfDNA compartment. B) A representative case showing an occult subclone harboring an ATP6V1B2 mutation only detected in the cfDNA compartment. Phylogenetic reconstruction shows that the bone marrow and cfDNA sample more readily predicts the genetic background of disease relapse two treatment lines later than nodal tisDNA.*

DOI:10.14753/SE.2025.3134

4.3.5. Prognostic value of ctDNA analysis in R/R FL

Median pretreatment ctDNA level was 1.44x10^3 human genomic equivalent/ml plasma. Investigating the prognostic value of pretreatment ctDNA level we found that treatment response in the subsequent treatment line was significantly associated with pretreatment ctDNA level (Figure 14.). On the other hand, pretreatment ctDNA level was not associated with inferior progression free survival (Figure 14).

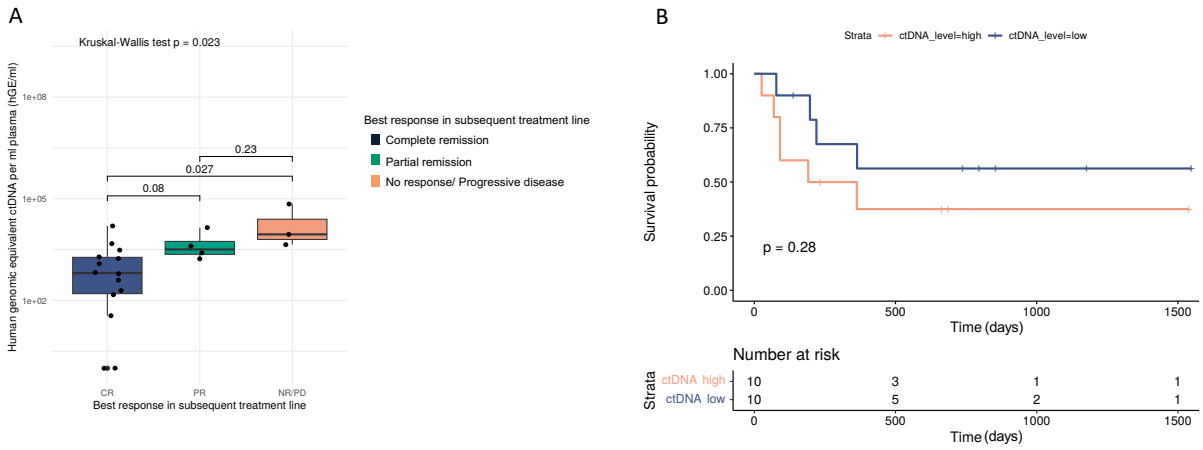

Figure 14. *Prognostic value of pretreatment ctDNA level in R/R FL. A) Pretreatment ctDNA level is significantly associated with treatment response in the subsequent treatment line. B) Pretreatment ctDNA level is not associated with progression free survival in our cohort.*

5. DISCUSSION

5.1. INVESTIGATION OF THE ROLE OF *TNFRSF14* AND *EZH2* IN THE PATHOGENESIS OF PCFCL

The aim of this *first* study was to better understand the genetic background of PCFCL by performing FISH analysis of the *BCL2* break and deletion of 1p36, and mutation analysis of the *TNFRSF14* and *EZH2* genes. We report for the first time mutations of the *TNFRSF14* gene occurring simultaneously with 1p36 deletion resulting in loss of functional copy of the gene. High EZH2 protein expression was found in about half of the PCFCL cases, while EZH2 hotspot mutations were not detected in our cohort.

We identified 1p36 deletion in 5/21 (22%) cases. Szablewski et al. were the first to report one case of PCFCL with 1p36 deletion in a cohort of 25 cases with 19 (76%) being BCL2 positive and 12 (48%) harboring BCL2 gene break (72). A more recent manuscript from the same group described 4 cases out of 29 (16.7%) positive for 1p36 deletion, but this cohort included only 14 (48%) BCL2 positive cases and 3 cases (11%) with BCL2 gene break (73). Our results are consistent with their findings, as our cohort included 10 (47%) cases positive for BCL2, and we identified BCL2 gene break in 2 out of 20 cases (10%). In both cohorts, 1p36 deletion was more common than BCL2 break: 22% compared to 10 and 16.7% compared to 11%, respectively, and the ratio of BCL2 positive tumors was also comparable (47 vs. 48%). These genetic abnormalities were mutually exclusive, while in FL, 1p36 deletion was the most common secondary cytogenetic lesion besides the t(14;18) translocation. Based on this observation, FISH examination of the *BCL2* translocation and 1p36 deletion may be applied as a differential diagnostic tool to distinguish primary cutaneous and nodal FL involving the skin. Cytogenetic abnormalities in our series did not show any association with morphological features and disease outcome, although, relapse tended to occur in shorter time for cases with cytogenetic aberrations and the only case with systemic dissemination also carried a deletion of 1p36. Multiple lesions were found significantly more often at diagnosis in cases with *BCL2* break or 1p36 deletion. Vernadet et al. found comparable results with no significant effect of cytogenetic aberrations on disease outcome; however, CR was achieved less frequently in cases of PCFCL with cytogenetic aberrations compared to those without chromosomal abnormalitites (73). In their study, disease stage at diagnosis was not defined. *BCL2* break itself did not show association with clinical outcome in most

studies on PCFCL; however, Ledard et al. observed association of extranodal dissemination with *BCL2* translocation (74). Data on the prognostic significance of cytogenetic alterations in FL are controversial: Cheng et al. described FL cases with 1p36 deletions associated with poor prognosis, but others found no association with clinical outcome (45, 69). Immunohistochemistry revealed BCL2 expression in 48% of our cases, with a tendency to correlate with low proliferation rate and small cell morphology. This can be explained by the fact that, FLs with high BCL2 expression gain resistance to apoptosis and can expand with low proliferation rate, while BCL2 negative FL need high proliferation rates to expand. BCL2 positivity ranged from 12 to 75% of the reported cases in the literature (73, 75-77). The discrepancy might be caused by using different antibodies or by the method evaluating the BCL2 immunostaining. High frequency of BCL2 protein expression was also observed in t(14;18) negative FL, indicating other mechanisms than BCL2 gene translocation for protein overexpression in the germinal center derived tumor cells. BCL2 amplification could be one, but this abnormality has been seldom reported and we did not observe BCL2 amplification in our cases (76). Next, we hypothesized that other mechanisms than 1p36 deletion could lead to the inactivation of *TNFRSF14*, so we investigated the possibility of *TNFRSF14* gene inactivation by somatic mutations in PCFCL. We identified 4 cases out of 17 harboring two types of mutations in the *TNFRSF14* gene. Three patients had c.35G > A; p.Trp12* mutation that was previously described by Cheung et al. in FL (69). We are the first to report a mutation occurring in exon 2 (c.157 T > G; p. Cys53Gly) possibly affecting the protein function. Two of the four mutant cases had concomitant 1p36 deletion leading to complete loss of functional *TNFRSF14*. The tumor suppressor role of *TNFRSF14* gene was suggested based on earlier observations on lymphoma and adenocarcinoma cell lines and was confirmed by recent studies on FL (78). High rate of partial or complete loss of functional *TNFRSF14* gene by deletion and/or somatic mutations was described in classical FL by several authors, and *TNFRSF14* mutations were accompanied by copy number neutral loss of heterozygosity of the 1p36 locus in over 70% of mutated cases in pediatric-type FL, that is a t(14;18) negative variant of FL with low genetic complexity and excellent clinical outcome (45, 69, 79). Significant impact of mutations on disease outcome of our four patients with *TNFRSF14* gene was not observed. We performed mutation analysis of the histone methyltransferase *EZH2* at three known mutation hotspots and assessed the

EZH2 protein expression using immunohistochemistry. While all cases were wild type for the hotspots analyzed, about half of the cases (52%) expressed high levels of EZH2 protein, and this was strongly associated with BCL2 negativity. However, we did not find correlation between EZH2 and Ki67 expression. High EZH2 expression was found to correlate with high proliferation rate in DLBCL and also in T-cell neoplasms, but not with BCL2 expression (80, 81). High EZH2 expression was shown to be a good prognostic factor for ABC-type DLBCL in another study (82). We did not find any correlation between the EZH2 expression and clinical outcome in our PCFCL cohort.

5.2. ANALYSIS OF COPY NUMBER ALTERATIONS IN PCFCL USING LOW-COVERAGE WGS

The different genetic background of PCFCL than FL was highlighted by early studies. Including our *first* study, sequencing studies identified lower prevalence of somatic variants in epigenetic modifiers in the disease including *KMT2D*, *CREBBP* and *EZH2* than observed in FL, but similar prevalence of mutations in immunoregulatory genes, including *TNFRSF14*, *STAT6*, *FOXO1* and *TNFAIP3* (39, 40). Differential diagnostic and prognostic models partly shifted from cytogenetic alterations to somatic variants. Recently, somatic variants in epigenetic modifiers and *IGH::BCL2* rearrangement have been integrated in a risk prediction algorithm for differentiating PCFCL from secondary cutaneous spread of FL and PCFCL with later systemic propagation (39).

Despite emerging data on short variants, genome-wide copy number profiles were only available for 54 PCFCL patients from six different studies using array CGH (39, 83-87). These studies compared PCFCL to secondary cutaneous spread of FL for differential diagnosis or PCFCL with large cells to PCDLBCL, leg-type to uncover the prognostic significance of alterations and to confirm the classification. Additionally, in our *first* study we detected ongoing BCL2 expression despite the lack of *IGH::BCL2* translocation in the majority of the cases, and EZH2 overexpression in more than half of the cases warranting further research for underlying genetic mechanisms.

Using lcWGS, we identified copy number alterations in 26 of 28 PCFCL samples from 20 patients, with the most frequent deletions affecting chromosome arms 1p, 6q and chromosome 19, and amplifications emerging on 1q, 2p and 12q, which altogether is in line with previous data from cutaneous B-cell lymphomas (39, 83-85) and constitute a

similar pattern to that of FL (88, 89). Notably, in our cohort focal and gross 6q deletions were identified in up to 14.3% and 10.7% of the samples, respectively, which has been previously implicated as a distinctive feature of leg-type PCDLBCL-s compared to PCFCL large cells in a patient cohort with similar size (86).

We systematically compared the copy number distribution of PCFCL to a process matched cohort of FL cases, which revealed significant enrichment of amplifications on the 18q chromosome arm in FL, peaking at 18q21.33 covering *BCL2*, while 13q14.11-q14.2 amplifications involving *FOXO1* were enriched in PCFCL. Amplifications on chromosome 18 were described to be present in around 25% of FL cases and provide complementary genetic basis for the activation of *BCL2* both with and without *IGH::BCL2* rearrangement (88, 90). Additionally, amplifications on chromosome 18 can play a role in the activation of *MALT1* and *PMAIP1 (91)*. Comparing 9 PCFCL and 13 leg-type PCLBCL cases, Hallermann and colleagues have shown, that chromosome 18 amplifications were the most common CNAs across all cutaneous B-cell lymphomas in their cohort (8/22), yet it was exclusively limited to PCDLBCL and were absent from PCFCL cases (85). Our results underline the fact that *BCL2* amplification has a minor role in PCFCL pathogenesis in contrast to FL and provide evidence in line with literature data, that amplification on chromosome 18 can be analyzed for differential diagnostic purposes, potentially both differentiating PCFCL from FL and PCDLBCL. Based on our results, 2p22.2-p15 amplification had a higher frequency in PCFCL samples displaying detectable BCL2 expression. The amplification potentially leads to *REL* overexpression and thus activation of the NF-kB pathway (92), which may enhance the expression of BCL2 in the absence of *IGH::BCL2* translocation or 18q21.33 amplification.

Amplification of the 13q14.11-q14.2 region, described in 15.0% of our cohort, has not yet been described as a recurrent CNA in lymphomas. The most reasonable candidate gene for the amplified region would be *FOXO1*, functioning as a transcriptional regulator and known to harbor recurrent oncogenic hotspot mutations in lymphomas enabling nuclear retention and avoidance of cytoplasmic inactivation (93).

Investigating the role of CNAs in disease progression revealed a higher prevalence of 1p36.23-p22 deletions in recurrence samples and these were more frequent in cases developing distant disease spread during the disease course. Deletions of this region were

not previously implicated in the pathogenesis of lymphomas. In all but one case, it occurred together with the p terminal deletion of 1p36, yet its emergence as a sole event in patient #16 points to a potential role in pathogenesis. The region encompasses the coding sequences of *MTOR*, *TNFRSF8 (CD30)* and *TNFRSF1B,* which are described to have an activating role in a majority of other lymphomas (94-96), potentially suggesting a pleiotropic effect of these genes in lymphomagenesis.

Disease recurrence in PCFCL is mainly localized to the surgical bed or anatomic region (27). Distant cutaneous and extracutaneous spread can increase subjective disease burden and suggests different biological background of disease spread. Previously, a higher number of genomic imbalances was observed in PCDLBCL than in PCFCL large cells (84, 85), yet its prognostic role has never been investigated in PCFCL. In our series, both proportion of the altered genome and number of CNAs were higher in patients developing distant spread pointing to increased genomic instability in tumor samples of these patients. Investigating the role of distinct CNAs in disease propagation revealed that distant recurrence was highly associated with 2p amplifications peaking at the 2p15 cytoband, present in 4/5 patients at their first presentation and in 6/10 samples of patients developing distant recurrence. Furthermore, 2p amplifications were present in all samples of case #12 and #20, suggesting the acquisition of 2p amplification in the earliest common progenitor leading to systemic involvement and soft tissue infiltration with high-grade morphology. The significantly enriched regions from 2p22.3-p15 are spanning the coding regions of *XPO1*, *REL*, *FBXO1* and *BIRC6*, respectively. An important target of the region is *REL* in 2p16.1, which is a transcriptional regulator as a subunit of NF-kB harboring a central role in BCR signaling and malignant transformation. In early studies investigating FL, *REL* amplifications were described only in cases undergoing high grade transformation (99, 100), but this was refined in later studies, also reporting amplifications in low grade cases, yet with a slightly lower prevalence (89, 101). Amplifications involving the locus of *REL* on 2p have been described in two studies as the most prevalent CNA in PCFCL with large cells, similar to our case #20 (85, 86), but were absent from other studies (83, 84, 87). Another important target in this region is *XPO1* on 2p15, in which the p.E571K activating mutation has been described in classical Hodgkin lymphoma and primary mediastinal B-cell lymphoma with a prevalence of 25% (102). Activation of XPO1 leads to abnormal nuclear export resulting in the abnormal

intracellular distribution of DNA damage control proteins and cell cycle regulators. Although, recurrent hotspot mutations were absent in other germinal center lymphomas, recurrent amplifications have been described in DLBCL and PMBL, where those correlated with increased levels of the respective mRNA (102, 103). Including all samples, 3q23-q24 amplification and 6q16.1-q23.3 deletion, as well as 9p21.3 deletion were more frequently observed in samples from PCFCL patients developing distant recurrence. Amplifications of 3q have only been described in one of the seminal studies and were restricted to leg-type DLBCL cases (83). Deletions of the 6q chromosome arm were specific to PCDLBCL in a previous study comparing PCDLBCL to PCFCL, large cells, potentially explaining the increased tendency of distant spread in samples harboring this alteration. 6q deletions lead to the loss of crucial tumor suppressor genes and immune regulators in the pathogenesis of mature lymphoid malignancies including *PRDM1*, *SGK1* and *TNFAIP3 (86)*. Deletions of 9p21.3 were thought to be characteristic of leg-type DLBCL and conferring dismal prognosis (84, 86, 104). The exclusive occurrence of 9p21.3 deletion in PCDLBCL leg-type was described in cohorts with limited case numbers encompassing 6/6 and 5/12 9p21.3 deletion positive PCDLBCL, as well as 0/4 and 0/19 9p21.3 deleted PCFCL cases (84, 86). Using a higher resolution multiplex ligation-dependent probe amplification method, reanalysis of a subset of previously 9p21.3 negative cases in one of the studies revealed a single PCFCL case harboring a hemizygous 9p21.3 deletion (86, 104). We identified 9p21.3 deletions in 4/28 samples from 2 patients. Case #11 acquired 9p21.3 deletion at third recurrence affecting the head and neck region and showing small cell morphology. Case #20 had a detectable 9p21.3 deletion in the primary sample from the left lower arm, which later recurred in the legs as a fast-growing thick subcutaneous tumor with large cell morphology, 80-90% cell proliferation rate and soft tissue involvement. Intriguingly, the 9p21.3 deleted subclone was eliminated by chemoimmunotherapy and it was undetectable from the last recurrence sample with small cell morphology.

For the first time, we investigated spatiotemporal dynamics of genome-wide CNAs in PCFCL patients using consecutive samples from 6 patients, with 3 patients showing an overlapping copy number profile. Interestingly, clonally unrelated relapses were also detected in case #5.

Progressive clinical course occurred in 2 of the 6 cases. During disease propagation, expansion of different subclones were observed in both cases, with unique CNAs found in all samples pointing to remarkable evolutionary plasticity of CNAs in PCFCL. In case #12 showing systemic progression, the common precursor harbored an arm level 2p and focal 1q and 12q amplifications, which have been known to play an established role in FL pathogenesis (89) and additionally acquired a focal gain in the centromeric region of chromosome 1, as well as a focal 7q11.21-q11.23 deletion during propagation to FL. In case #20, focal deletion of 6q16.1-q24.1 found in the common precursor was previously associated with shorter overall survival in FL (89) and with the diagnosis of PCDLBCL (19). During disease propagation, a subclone harboring a 9p21.3 deletion previously associated with high-grade transformation of FL and also a characteristic feature of PCDLBCL expanded, which was followed by the acquisition of a 3q25.1-q29 amplification detected in the sample with the most aggressive morphology, potentially further supporting the role of these genetic changes in PCFCL progression (89). Notably, the copy number profile of the case developing systemic spread included CNAs significantly associated with distant cutaneous spread in our analysis. However, as this observation is based only on a single case with systemic spread, it remains to be further investigated whether there is a link in pathogenesis between cases showing distant cutaneous spread and systemic propagation.

5.3. INVESTIGATION OF SPATIAL GENETIC HETEROGENEITY IN R/R FL ANALYZING CONCURRENT CELL-FREE DNA – TISSUE DNA PAIRS

In this study, we investigated intrapatient genetic heterogeneity in R/R FL applying comprehensive genetic profiling on concurrent tisDNA and cfDNA samples, as well as sequential samples across treatment lines. In our clinically high-risk cohort, most frequent alterations were identified in *KMT2D*, *CREBBP* and *TNFRSF14* in line with literature data (36, 64, 105, 106). Variants could be detected in 87.5% (21/24) of pretreatment cfDNA samples with median 7 variants per sample similarly to a previous study in frontline FL, where median 6.71 mutations were detected in 67.9% (18/29) of baseline patient samples (51). Using different variant filtering methods we could estimate the technical and biological components of intrapatient genetic heterogeneity. While using tumor-naïve filtering of variants resulted in median 44.4% overlap of non-silent variants

in cfDNA-tisDNA pairs, using tumor informed filtering this could be increased to 63.6%. A plateau was reached when we only retained positions with ultra-deep sequencing depth in all samples at 69.0%, suggesting an additional 30% contribution of biological determinants to observed intrapatient heterogeneity. Notably, we observed a marked patient-to-patient, and if available an intrapatient variation in cfDNA-tisDNA concordance further underlining the role of patient and sample specific biological factors in intrapatient genetic heterogeneity, a number of which is yet to be investigated. Although the variations in laboratory and informatic workflows make it difficult to compare concordance values across studies, in previous studies the observed concordance of cfDNA-tisDNA sample pairs varied between 31-67% of variants (51, 52, 107). Although the far from total concordance has been known since the first cfDNA studies, direct evidence for the origin of discordant alterations have scarcely been shown in B-cell lymphomas (49). Investigating spatial dynamics of subclones revealed two patterns of spatial heterogeneity that can be resolved by cfDNA profiling. The first pattern was identified in 4/5 patients with sample triplicates from the same timepoint, showing that multiregional sequencing can identify spatially restricted disease subclones, which are readily recovered using cfDNA analysis. As evidenced by phylogenetic reconstruction of the same patients' serial tumor samples throughout the disease course, these subclones can also drive disease relapse. The second pattern shows the existence of occult subclones only recoverable in the cfDNA compartment highlighting its potential usage in the molecular characterization of deep, visceral tumor sites. Although the cohort size in our study was limited, we further investigated the prognostic value of ctDNA level in the subsequent treatment line. In our R/R FL cohort treatment response in the subsequent treatment line was significantly associated with pretreatment ctDNA level, however, progression free survival was not different between patients stratified by median ctDNA level. So far only two studies focused on the prognostic of value of pretreatment ctDNA level. Pretreatment ctDNA level based on immunoglobulin high-throughput sequencing was associated with progression free survival (108). In frontline FL pretreatment ctDNA level based on farget-capture sequencing, as well as number of variants were significantly associated with treatment response and POD24 status (51).

DOI:10.14753/SE.2025.3134

6. CONCLUSIONS

Novel findings of my thesis are the following:

1. We observed *TNFRSF14* mutations in PCFCL and identified PCFCL cases with complete loss of functional *TNFRSF14* as a consequence of combined 1p36 loss and *TNFRSF14* mutation for the first time.
2. We demonstrated the feasibility of lcWGS for the genome-wide copy number profiling in indolent lymphomas for the first time in a cohort of 28 PCFCL and 64 FL samples.
3. We identified differential distribution of 18q21.33 amplification, 13q14.11-q14.2 deletion and 10q23.32 deletion between PCFCL and FL using lcWGS.
4. We observed for the first time, that higher copy number burden, including proportion of genome altered, as well as number of CNAs were significantly higher in patients developing distant cutaneous spread in PCFCL. Additionally, we identified 2p22.2-p15, 12q13.13-q14.3 and 3q23-q24 amplifications and 9p21.3 deletions as potential biomarkers of distant cutaneous spread.
5. We identified 2p22.2-p15 amplification as an early alteration associated with aggressive disease course analyzing serial tissue samples from six PCFCL patients.
6. We compared the concordance of somatic alterations in FL including cfDNA, lymph node, extranodal and bone marrow samples.
7. We demonstrated two patterns of subclonal dynamics using multiregional sequencing in FL including spatially restricted subclones and occult subclones only recoverable in cfDNA analysis clarifying the pathogenesis of observed discordance in cfDNA-tisDNA pairs in previous studies
8. We provided preliminary evidence that pretreatment ctDNA level has prognostic value in FL.

DOI:10.14753/SE.2025.3134

7. SUMMARY

Germinal center B cell lymphomas are the most prevalent hematologic malignancies representing diverse lymphoma subtypes. Herein, we aimed to investigate the genetic background of two indolent lymphoma subtypes, primary cutaneous follicle center lymphoma (PCFCL) and follicular lymphoma (FL). Both lymphomas are characterized by slow progression and long term remissions, although relapses develop in the majority of cases and a subset of patients experiences dismal prognosis posing a difficulty in clinical decision making due to the lack of reliable prognostic and predictive biomarkers. Altogether we investigated 227 biosamples from PCFCL and FL patients in three different studies. We aimed to investigate the role of TNFRSF14 and EZH2 in the pathogenesis of PCFCL and performed genome-wide copy number profiling using low-coverage whole genome sequencing to identify novel diagnostic and prognostic biomarkers in PCFCL. We aimed to investigate the potential of cell-free DNA analysis in FL and leverage its potential to uncover spatial heterogeneity in the disease.

In summary, findings of this study extend our knowledge on the genetic background of PCFCL, that seems to be heterogeneous. We identified for the first time somatic mutations of the *TNFRSF14* gene and/or 1p36 loss in the minority of the cases. Based on our results, the copy number profile of PCFCL is only slightly different from that of FL, with the notable exception of the scarcity of 18q amplifications including 18q21.33 which covers the *BCL2* locus. This further highlights its potential utility in differential diagnosis of PCFCL and secondary cutaneous infiltration of FL. Our results point to higher genomic instability in patients developing distant disease spread. We further deciphered the role of 2p16.3-p15 amplifications in the disease course of PCFCL, which could be an early prognostic marker in the future for the prediction of distant disease spread. For the first time, we analyzed the temporospatial plasticity of PCFCL investigating serial patient samples highlighting evidence of branching evolutionary processes during disease propagation. Additionally, performing comprehensive genetic profiling on concurrent and serial cell-free DNA and tumor DNA samples in relapsed/refractory FL cases we were able to decipher the spatial compartmentalization of variants including its dynamics leading to disease relapse and investigate the potential utility of circulating tumor DNA analysis in the risk stratification of FL.

8. REFERENCES

1. Silkenstedt E, Salles G, Campo E, Dreyling M. B-cell non-Hodgkin lymphomas. Lancet. 2024;403(10438):1791-807.

2. Alaggio R, Amador C, Anagnostopoulos I, Attygalle AD, Araujo IBO, Berti E, et al. The 5th edition of the World Health Organization Classification of Haematolymphoid Tumours: Lymphoid Neoplasms. Leukemia. 2022;36(7):1720-48.

3. Cerhan JR. Epidemiology of Follicular Lymphoma. Hematol Oncol Clin North Am. 2020;34(4):631-46.

4. Goodlad JR, MacPherson S, Jackson R, Batstone P, White J, Scotland, et al. Extranodal follicular lymphoma: a clinicopathological and genetic analysis of 15 cases arising at non-cutaneous extranodal sites. Histopathology. 2004;44(3):268-76.

5. Dreyling M, Ghielmini M, Rule S, Salles G, Ladetto M, Tonino SH, et al. Newly diagnosed and relapsed follicular lymphoma: ESMO Clinical Practice Guidelines for diagnosis, treatment and follow-up. Ann Oncol. 2021;32(3):298-308.

6. Salles GA. Clinical features, prognosis and treatment of follicular lymphoma. Hematology Am Soc Hematol Educ Program. 2007:216-25.

7. Swerdlow SH, Campo E, Pileri SA, Harris NL, Stein H, Siebert R, et al. The 2016 revision of the World Health Organization classification of lymphoid neoplasms. Blood. 2016;127(20):2375-90.

8. Network NCC. B-cell Lymphomas (Version 2.2024) [Available from: https://www.nccn.org/professionals/physician_gls/pdf/b-cell_blocks.pdf.

9. Junlen HR, Peterson S, Kimby E, Lockmer S, Linden O, Nilsson-Ehle H, et al. Follicular lymphoma in Sweden: nationwide improved survival in the rituximab era, particularly in elderly women: a Swedish Lymphoma Registry study. Leukemia. 2015;29(3):668-76.

10. Casulo C, Byrtek M, Dawson KL, Zhou X, Farber CM, Flowers CR, et al. Early Relapse of Follicular Lymphoma After Rituximab Plus Cyclophosphamide, Doxorubicin, Vincristine, and Prednisone Defines Patients at High Risk for Death: An Analysis From the National LymphoCare Study. J Clin Oncol. 2015;33(23):2516-22.

11. Bains P, Al Tourah A, Campbell BA, Pickles T, Gascoyne RD, Connors JM, et al. Incidence of transformation to aggressive lymphoma in limited-stage follicular lymphoma treated with radiotherapy. Ann Oncol. 2013;24(2):428-32.

12. Conconi A, Ponzio C, Lobetti-Bodoni C, Motta M, Rancoita PM, Stathis A, et al. Incidence, risk factors and outcome of histological transformation in follicular lymphoma. Br J Haematol. 2012;157(2):188-96.
13. Montoto S, Davies AJ, Matthews J, Calaminici M, Norton AJ, Amess J, et al. Risk and clinical implications of transformation of follicular lymphoma to diffuse large B-cell lymphoma. J Clin Oncol. 2007;25(17):2426-33.
14. Link BK, Maurer MJ, Nowakowski GS, Ansell SM, Macon WR, Syrbu SI, et al. Rates and outcomes of follicular lymphoma transformation in the immunochemotherapy era: a report from the University of Iowa/MayoClinic Specialized Program of Research Excellence Molecular Epidemiology Resource. J Clin Oncol. 2013;31(26):3272-8.
15. Al-Tourah AJ, Gill KK, Chhanabhai M, Hoskins PJ, Klasa RJ, Savage KJ, et al. Population-based analysis of incidence and outcome of transformed non-Hodgkin's lymphoma. J Clin Oncol. 2008;26(32):5165-9.
16. Solal-Celigny P, Roy P, Colombat P, White J, Armitage JO, Arranz-Saez R, et al. Follicular lymphoma international prognostic index. Blood. 2004;104(5):1258-65.
17. Pastore A, Jurinovic V, Kridel R, Hoster E, Staiger AM, Szczepanowski M, et al. Integration of gene mutations in risk prognostication for patients receiving first-line immunochemotherapy for follicular lymphoma: a retrospective analysis of a prospective clinical trial and validation in a population-based registry. Lancet Oncol. 2015;16(9):1111-22.
18. Carbone PP, Kaplan HS, Musshoff K, Smithers DW, Tubiana M. Report of the Committee on Hodgkin's Disease Staging Classification. Cancer Res. 1971;31(11):1860-1.
19. Brice P, Bastion Y, Lepage E, Brousse N, Haioun C, Moreau P, et al. Comparison in low-tumor-burden follicular lymphomas between an initial no-treatment policy, prednimustine, or interferon alfa: a randomized study from the Groupe d'Etude des Lymphomes Folliculaires. Groupe d'Etude des Lymphomes de l'Adulte. J Clin Oncol. 1997;15(3):1110-7.
20. Guadagnolo BA, Li S, Neuberg D, Ng A, Hua L, Silver B, et al. Long-term outcome and mortality trends in early-stage, Grade 1-2 follicular lymphoma treated with radiation therapy. Int J Radiat Oncol Biol Phys. 2006;64(3):928-34.

21. Solal-Celigny P, Bellei M, Marcheselli L, Pesce EA, Pileri S, McLaughlin P, et al. Watchful waiting in low-tumor burden follicular lymphoma in the rituximab era: results of an F2-study database. J Clin Oncol. 2012;30(31):3848-53.

22. Chen ST, Barnes J, Duncan L. Primary cutaneous B-cell lymphomas- clinical and histopathologic features, differential diagnosis, and treatment. Semin Cutan Med Surg. 2018;37(1):49-55.

23. Bradford PT, Devesa SS, Anderson WF, Toro JR. Cutaneous lymphoma incidence patterns in the United States: a population-based study of 3884 cases. Blood. 2009;113(21):5064-73.

24. Willemze R, Jaffe ES, Burg G, Cerroni L, Berti E, Swerdlow SH, et al. WHO-EORTC classification for cutaneous lymphomas. Blood. 2005;105(10):3768-85.

25. Smith BD, Smith GL, Cooper DL, Wilson LD. The cutaneous B-cell lymphoma prognostic index: a novel prognostic index derived from a population-based registry. J Clin Oncol. 2005;23(15):3390-5.

26. Olsen EA, Whittaker S, Willemze R, Pinter-Brown L, Foss F, Geskin L, et al. Primary cutaneous lymphoma: recommendations for clinical trial design and staging update from the ISCL, USCLC, and EORTC. Blood. 2022;140(5):419-37.

27. Hamilton SN, Wai ES, Tan K, Alexander C, Gascoyne RD, Connors JM. Treatment and outcomes in patients with primary cutaneous B-cell lymphoma: the BC Cancer Agency experience. Int J Radiat Oncol Biol Phys. 2013;87(4):719-25.

28. Willemze R, Hodak E, Zinzani PL, Specht L, Ladetto M, Committee EG. Primary cutaneous lymphomas: ESMO Clinical Practice Guidelines for diagnosis, treatment and follow-up. Ann Oncol. 2018.

29. Network NCC. Primary Cutaneous Lymphomas (Version 2.2024) [Available from: https://www.nccn.org/professionals/physician_gls/pdf/primary_cutaneous.pdf.

30. Hoefnagel JJ, Dijkman R, Basso K, Jansen PM, Hallermann C, Willemze R, et al. Distinct types of primary cutaneous large B-cell lymphoma identified by gene expression profiling. Blood. 2005;105(9):3671-8.

31. Gatto D, Brink R. The germinal center reaction. J Allergy Clin Immunol. 2010;126(5):898-907; quiz 8-9.

32. Garcillan B, Figgett WA, Infantino S, Lim EX, Mackay F. Molecular control of B-cell homeostasis in health and malignancy. Immunol Cell Biol. 2018;96(5):453-62.

33. Huet S, Sujobert P, Salles G. From genetics to the clinic: a translational perspective on follicular lymphoma. Nat Rev Cancer. 2018;18(4):224-39.

34. Morin RD, Mendez-Lago M, Mungall AJ, Goya R, Mungall KL, Corbett RD, et al. Frequent mutation of histone-modifying genes in non-Hodgkin lymphoma. Nature. 2011;476(7360):298-303.

35. Bodor C, Grossmann V, Popov N, Okosun J, O'Riain C, Tan K, et al. EZH2 mutations are frequent and represent an early event in follicular lymphoma. Blood. 2013;122(18):3165-8.

36. Okosun J, Bodor C, Wang J, Araf S, Yang CY, Pan C, et al. Integrated genomic analysis identifies recurrent mutations and evolution patterns driving the initiation and progression of follicular lymphoma. Nat Genet. 2014;46(2):176-81.

37. Ortega-Molina A, Boss IW, Canela A, Pan H, Jiang Y, Zhao C, et al. The histone lysine methyltransferase KMT2D sustains a gene expression program that represses B cell lymphoma development. Nat Med. 2015;21(10):1199-208.

38. Zhang J, Dominguez-Sola D, Hussein S, Lee JE, Holmes AB, Bansal M, et al. Disruption of KMT2D perturbs germinal center B cell development and promotes lymphomagenesis. Nat Med. 2015;21(10):1190-8.

39. Zhou XA, Yang J, Ringbloom KG, Martinez-Escala ME, Stevenson KE, Wenzel AT, et al. Genomic landscape of cutaneous follicular lymphomas reveals 2 subgroups with clinically predictive molecular features. Blood Adv. 2021;5(3):649-61.

40. Barasch NJK, Liu YC, Ho J, Bailey N, Aggarwal N, Cook JR, et al. The molecular landscape and other distinctive features of primary cutaneous follicle center lymphoma. Hum Pathol. 2020;106:93-105.

41. Jiang Y, Ortega-Molina A, Geng H, Ying HY, Hatzi K, Parsa S, et al. CREBBP Inactivation Promotes the Development of HDAC3-Dependent Lymphomas. Cancer Discov. 2017;7(1):38-53.

42. Bodor C, Grossmann V, Popov N, Okosun J, O'Riain C, Tan K, et al. EZH2 mutations are frequent and represent an early event in follicular lymphoma. Blood. 2013;122(18):3165-8.

43. Sneeringer CJ, Scott MP, Kuntz KW, Knutson SK, Pollock RM, Richon VM, et al. Coordinated activities of wild-type plus mutant EZH2 drive tumor-associated

hypertrimethylation of lysine 27 on histone H3 (H3K27) in human B-cell lymphomas. Proc Natl Acad Sci U S A. 2010;107(49):20980-5.

44. Bátai B, Lévai, D., Gaál-Weisinger, J., Balogh, A., Gángó, A., Bödör, Cs., Nagy, N. A személyre szabott terápia új lehetősége follicularis lymphomában – Az EZH2 hiszton metil-transzferáz gátlása [New perspective in the personalized medicine of follicular lymphoma – Targeting the EZH2 histone methyltransferase]. Hematológia-Transzfuziológia. 2018;51(2):61-70.

45. Launay E, Pangault C, Bertrand P, Jardin F, Lamy T, Tilly H, et al. High rate of TNFRSF14 gene alterations related to 1p36 region in de novo follicular lymphoma and impact on prognosis. Leukemia. 2012;26(3):559-62.

46. Boice M, Salloum D, Mourcin F, Sanghvi V, Amin R, Oricchio E, et al. Loss of the HVEM Tumor Suppressor in Lymphoma and Restoration by Modified CAR-T Cells. Cell. 2016;167(2):405-18 e13.

47. Scheinin I, Sie D, Bengtsson H, van de Wiel MA, Olshen AB, van Thuijl HF, et al. DNA copy number analysis of fresh and formalin-fixed specimens by shallow whole-genome sequencing with identification and exclusion of problematic regions in the genome assembly. Genome Res. 2014;24(12):2022-32.

48. Cherng HJ, Sun R, Sugg B, Irwin R, Yang H, Le CC, et al. Risk assessment with low-pass whole-genome sequencing of cell-free DNA before CD19 CAR T-cell therapy for large B-cell lymphoma. Blood. 2022;140(5):504-15.

49. Scherer F, Kurtz DM, Newman AM, Stehr H, Craig AF, Esfahani MS, et al. Distinct biological subtypes and patterns of genome evolution in lymphoma revealed by circulating tumor DNA. Sci Transl Med. 2016;8(364):364ra155.

50. Schroers-Martin JG, Alig S, Garofalo A, Tessoulin B, Sugio T, Alizadeh AA. Molecular Monitoring of Lymphomas. Annu Rev Pathol. 2023;18:149-80.

51. Fernandez-Miranda I, Pedrosa L, Llanos M, Franco FF, Gomez S, Martin-Acosta P, et al. Monitoring of Circulating Tumor DNA Predicts Response to Treatment and Early Progression in Follicular Lymphoma: Results of a Prospective Pilot Study. Clin Cancer Res. 2023;29(1):209-20.

52. Jimenez-Ubieto A, Poza M, Martin-Munoz A, Ruiz-Heredia Y, Dorado S, Figaredo G, et al. Real-life disease monitoring in follicular lymphoma patients using liquid biopsy ultra-deep sequencing and PET/CT. Leukemia. 2023;37(3):659-69.

53. Nagy A, Batai B, Kiss L, Grof S, Kiraly PA, Jona A, et al. Parallel testing of liquid biopsy (ctDNA) and tissue biopsy samples reveals a higher frequency of EZH2 mutations in follicular lymphoma. J Intern Med. 2023.

54. Kurtz DM, Scherer F, Jin MC, Soo J, Craig AFM, Esfahani MS, et al. Circulating Tumor DNA Measurements As Early Outcome Predictors in Diffuse Large B-Cell Lymphoma. J Clin Oncol. 2018;36(28):2845-53.

55. Spina V, Bruscaggin A, Cuccaro A, Martini M, Di Trani M, Forestieri G, et al. Circulating tumor DNA reveals genetics, clonal evolution, and residual disease in classical Hodgkin lymphoma. Blood. 2018;131(22):2413-25.

56. Kurtz DM, Soo J, Co Ting Keh L, Alig S, Chabon JJ, Sworder BJ, et al. Enhanced detection of minimal residual disease by targeted sequencing of phased variants in circulating tumor DNA. Nat Biotechnol. 2021;39(12):1537-47.

57. Lakhotia R, Melani C, Dunleavy K, Pittaluga S, Saba N, Lindenberg L, et al. Circulating tumor DNA predicts therapeutic outcome in mantle cell lymphoma. Blood Adv. 2022;6(8):2667-80.

58. Kim YH, Willemze R, Pimpinelli N, Whittaker S, Olsen EA, Ranki A, et al. TNM classification system for primary cutaneous lymphomas other than mycosis fungoides and Sezary syndrome: a proposal of the International Society for Cutaneous Lymphomas (ISCL) and the Cutaneous Lymphoma Task Force of the European Organization of Research and Treatment of Cancer (EORTC). Blood. 2007;110(2):479-84.

59. Swerdlow SH, Campo E, Harris NL, Jaffe ES, Pileri SA, Stein H, et al. World Health Organization classification of Tumours of Haematopoietic and Lymphoid Tissues. 2017;Revised 4th edition(IARC).

60. Langerak AW, Groenen PJ, Bruggemann M, Beldjord K, Bellan C, Bonello L, et al. EuroClonality/BIOMED-2 guidelines for interpretation and reporting of Ig/TCR clonality testing in suspected lymphoproliferations. Leukemia. 2012;26(10):2159-71.

61. Papp G, Mihaly D, Sapi Z. Unusual Signal Patterns of Break-apart FISH Probes Used in the Diagnosis of Soft Tissue Sarcomas. Pathol Oncol Res. 2017;23(4):863-71.

62. van Beers EH, Joosse SA, Ligtenberg MJ, Fles R, Hogervorst FB, Verhoef S, et al. A multiplex PCR predictor for aCGH success of FFPE samples. Br J Cancer. 2006;94(2):333-7.

63. Pasqualucci L, Khiabanian H, Fangazio M, Vasishtha M, Messina M, Holmes AB, et al. Genetics of follicular lymphoma transformation. Cell Rep. 2014;6(1):130-40.

64. Kridel R, Chan FC, Mottok A, Boyle M, Farinha P, Tan K, et al. Histological Transformation and Progression in Follicular Lymphoma: A Clonal Evolution Study. PLoS Med. 2016;13(12):e1002197.

65. Bouska A, Zhang W, Gong Q, Iqbal J, Scuto A, Vose J, et al. Combined copy number and mutation analysis identifies oncogenic pathways associated with transformation of follicular lymphoma. Leukemia. 2017;31(1):83-91.

66. Gonzalez-Rincon J, Mendez M, Gomez S, Garcia JF, Martin P, Bellas C, et al. Unraveling transformation of follicular lymphoma to diffuse large B-cell lymphoma. PLoS One. 2019;14(2):e0212813.

67. Stewart JP, Gazdova J, Darzentas N, Wren D, Proszek P, Fazio G, et al. Validation of the EuroClonality-NGS DNA capture panel as an integrated genomic tool for lymphoproliferative disorders. Blood Adv. 2021;5(16):3188-98.

68. Gango A, Batai B, Varga M, Kapczar D, Papp G, Marschalko M, et al. Concomitant 1p36 deletion and TNFRSF14 mutations in primary cutaneous follicle center lymphoma frequently expressing high levels of EZH2 protein. Virchows Arch. 2018;473(4):453-62.

69. Cheung KJ, Johnson NA, Affleck JG, Severson T, Steidl C, Ben-Neriah S, et al. Acquired TNFRSF14 mutations in follicular lymphoma are associated with worse prognosis. Cancer Res. 2010;70(22):9166-74.

70. Batai B, Kiss L, Varga L, Nagy A, Househam J, Baker AM, et al. Profiling of Copy Number Alterations Using Low-Coverage Whole-Genome Sequencing Informs Differential Diagnosis and Prognosis in Primary Cutaneous Follicle Center Lymphoma. Mod Pathol. 2024;37(5):100465.

71. Bence Bátai, Ákos Nagy, Tibor Nagy, Gábor Bedics, Bence Gálik, Luca Varga, et al. Concurrent Testing of Spatially Separated Tissue Samples and Circulating Tumor DNA Reveals Substantial Intra-Patient Genetic Heterogeneity in Relapsed/Refractory Follicular Lymphoma. Blood. 2023;142(1):171-3.

72. Szablewski V, Ingen-Housz-Oro S, Baia M, Delfau-Larue MH, Copie-Bergman C, Ortonne N. Primary Cutaneous Follicle Center Lymphomas Expressing BCL2 Protein

Frequently Harbor BCL2 Gene Break and May Present 1p36 Deletion: A Study of 20 Cases. Am J Surg Pathol. 2016;40(1):127-36.

73. Verdanet E, Dereure O, Rene C, Tempier A, Benammar-Hafidi A, Gallo M, et al. Diagnostic value of STMN1, LMO2, HGAL, AID expression and 1p36 chromosomal abnormalities in primary cutaneous B cell lymphomas. Histopathology. 2017;71(4):648-60.

74. Pham-Ledard A, Cowppli-Bony A, Doussau A, Prochazkova-Carlotti M, Laharanne E, Jouary T, et al. Diagnostic and prognostic value of BCL2 rearrangement in 53 patients with follicular lymphoma presenting as primary skin lesions. Am J Clin Pathol. 2015;143(3):362-73.

75. Streubel B, Scheucher B, Valencak J, Huber D, Petzelbauer P, Trautinger F, et al. Molecular cytogenetic evidence of t(14;18)(IGH;BCL2) in a substantial proportion of primary cutaneous follicle center lymphomas. Am J Surg Pathol. 2006;30(4):529-36.

76. Abdul-Wahab A, Tang SY, Robson A, Morris S, Agar N, Wain EM, et al. Chromosomal anomalies in primary cutaneous follicle center cell lymphoma do not portend a poor prognosis. J Am Acad Dermatol. 2014;70(6):1010-20.

77. Lawnicki LC, Weisenburger DD, Aoun P, Chan WC, Wickert RS, Greiner TC. The t(14;18) and bcl-2 expression are present in a subset of primary cutaneous follicular lymphoma: association with lower grade. Am J Clin Pathol. 2002;118(5):765-72.

78. Costello RT, Mallet F, Barbarat B, Schiano De Colella JM, Sainty D, Sweet RW, et al. Stimulation of non-Hodgkin's lymphoma via HVEM: an alternate and safe way to increase Fas-induced apoptosis and improve tumor immunogenicity. Leukemia. 2003;17(12):2500-7.

79. Schmidt J, Gong S, Marafioti T, Mankel B, Gonzalez-Farre B, Balague O, et al. Genome-wide analysis of pediatric-type follicular lymphoma reveals low genetic complexity and recurrent alterations of TNFRSF14 gene. Blood. 2016;128(8):1101-11.

80. Zhou Z, Gao J, Popovic R, Wolniak K, Parimi V, Winter JN, et al. Strong expression of EZH2 and accumulation of trimethylated H3K27 in diffuse large B-cell lymphoma independent of cell of origin and EZH2 codon 641 mutation. Leuk Lymphoma. 2015;56(10):2895-901.

81. Shi M, Shahsafaei A, Liu C, Yu H, Dorfman DM. Enhancer of zeste homolog 2 is widely expressed in T-cell neoplasms, is associated with high proliferation rate and

correlates with MYC and pSTAT3 expression in a subset of cases. Leuk Lymphoma. 2015;56(7):2087-91.

82. Lee HJ, Shin DH, Kim KB, Shin N, Park WY, Lee JH, et al. Polycomb protein EZH2 expression in diffuse large B-cell lymphoma is associated with better prognosis in patients treated with rituximab, cyclophosphamide, doxorubicin, vincristine and prednisone. Leuk Lymphoma. 2014;55(9):2056-63.

83. Mao X, Lillington D, Child F, Russell-Jones R, Young B, Whittaker S. Comparative genomic hybridization analysis of primary cutaneous B-cell lymphomas: identification of common genomic alterations in disease pathogenesis. Genes Chromosomes Cancer. 2002;35(2):144-55.

84. Belaud-Rotureau MA, Marietta V, Vergier B, Mainhaguiet G, Turmo M, Idrissi Y, et al. Inactivation of p16INK4a/CDKN2A gene may be a diagnostic feature of large B cell lymphoma leg type among cutaneous B cell lymphomas. Virchows Arch. 2008;452(6):607-20.

85. Hallermann C, Kaune KM, Siebert R, Vermeer MH, Tensen CP, Willemze R, et al. Chromosomal aberration patterns differ in subtypes of primary cutaneous B cell lymphomas. J Invest Dermatol. 2004;122(6):1495-502.

86. Dijkman R, Tensen CP, Jordanova ES, Knijnenburg J, Hoefnagel JJ, Mulder AA, et al. Array-based comparative genomic hybridization analysis reveals recurrent chromosomal alterations and prognostic parameters in primary cutaneous large B-cell lymphoma. J Clin Oncol. 2006;24(2):296-305.

87. Gimenez S, Costa C, Espinet B, Sole F, Pujol RM, Puigdecanet E, et al. Comparative genomic hybridization analysis of cutaneous large B-cell lymphomas. Exp Dermatol. 2005;14(12):883-90.

88. Cheung KJ, Shah SP, Steidl C, Johnson N, Relander T, Telenius A, et al. Genome-wide profiling of follicular lymphoma by array comparative genomic hybridization reveals prognostically significant DNA copy number imbalances. Blood. 2009;113(1):137-48.

89. Bouska A, McKeithan TW, Deffenbacher KE, Lachel C, Wright GW, Iqbal J, et al. Genome-wide copy-number analyses reveal genomic abnormalities involved in transformation of follicular lymphoma. Blood. 2014;123(11):1681-90.

90. Galteland E, Sivertsen EA, Svendsrud DH, Smedshammer L, Kresse SH, Meza-Zepeda LA, et al. Translocation t(14;18) and gain of chromosome 18/BCL2: effects on BCL2 expression and apoptosis in B-cell non-Hodgkin's lymphomas. Leukemia. 2005;19(12):2313-23.

91. Sanchez-Izquierdo D, Buchonnet G, Siebert R, Gascoyne RD, Climent J, Karran L, et al. MALT1 is deregulated by both chromosomal translocation and amplification in B-cell non-Hodgkin lymphoma. Blood. 2003;101(11):4539-46.

92. Catz SD, Johnson JL. Transcriptional regulation of bcl-2 by nuclear factor kappa B and its significance in prostate cancer. Oncogene. 2001;20(50):7342-51.

93. Trinh DL, Scott DW, Morin RD, Mendez-Lago M, An J, Jones SJ, et al. Analysis of FOXO1 mutations in diffuse large B-cell lymphoma. Blood. 2013;121(18):3666-74.

94. Tensen CP, Quint KD, Vermeer MH. Genetic and epigenetic insights into cutaneous T-cell lymphoma. Blood. 2022;139(1):15-33.

95. Veyri M, Spano JP, Le Bras F, Marcelin AG, Todesco E. CD30 as a therapeutic target in adult haematological malignancies: Where are we now? Br J Haematol. 2023;201(6):1033-46.

96. Leseux L, Laurent G, Laurent C, Rigo M, Blanc A, Olive D, et al. PKC zeta mTOR pathway: a new target for rituximab therapy in follicular lymphoma. Blood. 2008;111(1):285-91.

97. Gruss HJ, Boiani N, Williams DE, Armitage RJ, Smith CA, Goodwin RG. Pleiotropic effects of the CD30 ligand on CD30-expressing cells and lymphoma cell lines. Blood. 1994;83(8):2045-56.

98. Sebestyen A, Sticz TB, Mark A, Hajdu M, Timar B, Nemes K, et al. Activity and complexes of mTOR in diffuse large B-cell lymphomas--a tissue microarray study. Mod Pathol. 2012;25(12):1623-8.

99. Nagy M, Balazs M, Adam Z, Petko Z, Timar B, Szereday Z, et al. Genetic instability is associated with histological transformation of follicle center lymphoma. Leukemia. 2000;14(12):2142-8.

100. Hough RE, Goepel JR, Alcock HE, Hancock BW, Lorigan PC, Hammond DW. Copy number gain at 12q12-14 may be important in the transformation from follicular lymphoma to diffuse large B cell lymphoma. Br J Cancer. 2001;84(4):499-503.

101. Kwiecinska A, Ichimura K, Berglund M, Dinets A, Sulaiman L, Collins VP, et al. Amplification of 2p as a genomic marker for transformation in lymphoma. Genes Chromosomes Cancer. 2014;53(9):750-68.

102. Jardin F, Pujals A, Pelletier L, Bohers E, Camus V, Mareschal S, et al. Recurrent mutations of the exportin 1 gene (XPO1) and their impact on selective inhibitor of nuclear export compounds sensitivity in primary mediastinal B-cell lymphoma. Am J Hematol. 2016;91(9):923-30.

103. Lenz G, Wright GW, Emre NC, Kohlhammer H, Dave SS, Davis RE, et al. Molecular subtypes of diffuse large B-cell lymphoma arise by distinct genetic pathways. Proc Natl Acad Sci U S A. 2008;105(36):13520-5.

104. Senff NJ, Zoutman WH, Vermeer MH, Assaf C, Berti E, Cerroni L, et al. Fine-mapping chromosomal loss at 9p21: correlation with prognosis in primary cutaneous diffuse large B-cell lymphoma, leg type. J Invest Dermatol. 2009;129(5):1149-55.

105. Krysiak K, Gomez F, White BS, Matlock M, Miller CA, Trani L, et al. Recurrent somatic mutations affecting B-cell receptor signaling pathway genes in follicular lymphoma. Blood. 2017;129(4):473-83.

106. Green MR, Kihira S, Liu CL, Nair RV, Salari R, Gentles AJ, et al. Mutations in early follicular lymphoma progenitors are associated with suppressed antigen presentation. Proc Natl Acad Sci U S A. 2015;112(10):E1116-25.

107. Nagy A, Batai B, Kiss L, Grof S, Kiraly PA, Jona A, et al. Parallel testing of liquid biopsy (ctDNA) and tissue biopsy samples reveals a higher frequency of EZH2 mutations in follicular lymphoma. J Intern Med. 2023;294(3):295-313.

108. Sarkozy C, Huet S, Carlton VE, Fabiani B, Delmer A, Jardin F, et al. The prognostic value of clonal heterogeneity and quantitative assessment of plasma circulating clonal IG-VDJ sequences at diagnosis in patients with follicular lymphoma. Oncotarget. 2017;8(5):8765-74.

DOI:10.14753/SE.2025.3134

9. BIBLIOGRAPHY OF THE CANDIDATE'S PUBLICATIONS

RELATED TO THE THESIS:

1, Bátai, B., Kiss, L., Varga, L., Nagy, Á., Househam, J., Baker, A-M., László, T., Udvari, A., Horváth, R., Nagy, T., Csomor, J., Szakonyi, J., Schneider, T., Graham, T.A., Alpár, D., Fitzgibbon, J., Szepesi, Á., Bödör, C. Profiling of copy number alterations using low-coverage whole-genome sequencing informs differential diagnosis and prognosis in primary cutaneous follicle center lymphoma, Modern Pathology 2024, 37(5): 100465.

2, Gango, A.*, Batai, B.*, Varga, M., Kapczar, D., Papp, G., Marschalko, M., Kuroli, E., Schneider, T., Csomor, J., Matolcsy, A., Bodor, C., Szepesi, A. Concomitant 1p36 deletion and TNFRSF14 mutations in primary cutaneous follicle center lymphoma frequently expressing high levels of EZH2 protein. Virchows Archiv 2018, 473(4): 453-462. *These two authors contributed equally to this work.

FURTHER PUBLICATIONS:

3, Bedics, G., Szőke, P., Bátai, B., Nagy, T., Papp, G., Kránitz, N., Rajnai, H., Reiniger, L., Bödör, Cs., Scheich, B. Novel, clinically relevant genomic patterns identified by comprehensive genomic profiling in ATRX-deficient IDH-wildtype adult high-grade gliomas. Scientific Reports. 2023;13(1):18436.

4, Bedics, G., Egyed, B., Kotmayer, L., Benard-Slagter, A., de Groot, K., Bekő, A., Hegyi, L. L., Bátai, B., Krizsán, Sz., Kriván, G., Erdélyi, D. J., Müller, J., Haltrich, I., Kajtár, B., Pajor, L., Vojcek, Á., Ottóffy, G., Ujfalusi, A., Szegedi, I., Tiszlavicz, L. Gy., Bartyik, K., Csanádi, K., Péter, Gy., Simon, R., Hauser, P., Kelemen, Á., Sebestyén, E., Jakab, Zs., Matolcsy, A., Kiss, Cs., Kovács, G., Savola, S., Bödör, Cs., Alpár, D. PersonALL: a genetic scoring guide for personalized risk assessment in pediatric B-cell precursor acute lymphoblastic leukemia. British Journal of Cancer. 2023; 129(3):455-465.

5, Nagy, Á., Bátai, B., Kiss, L., Gróf, S., Király, P. A., Jóna, Á., Demeter, J., Sánta, H., Bátai, Á., Pettendi, P., Szendrei, T., Plander, M., Körösmezey, G., Alizadeh, H., Kajtár, B., Méhes, G., Krenács, L, Timár, B., Csomor, J., Tóth, E., Schneider, T., Mikala, G., Matolcsy, A., Alpár, D., Masszi, A.*, Bödör, Cs.* Parallel testing of liquid biopsy (ctDNA) and tissue biopsy samples reveals a higher frequency of EZH2 mutations in follicular lymphoma. Journal of Internal Medicine. 2023; 294: 295–313.

6, Varga, A., Nguyen, M. T., Pénzes, K., Bátai, B., Gyulavári, P., Gurbi, B., Murányi, J., Csermely, P., Csala, M., Vántus, T., Sőti, Cs. Protein Kinase D3 (PKD3) Requires Hsp90 for Stability and Promotion of Prostate Cancer Cell Migration. Cells. 2023, 12(2), 212.

7, Nagy, Á., Bátai, B., Balogh, A., Illés, S., Mikala, G., Nagy, N., Kiss, L., Kotmayer, L., Matolcsy, A., Alpár, D., Masszi, T., Masszi, A., Bödör Cs. Quantitative Analysis and Monitoring of EZH2 Mutations Using Liquid Biopsy in Follicular Lymphoma. Genes (Basel) 2020, 11(7): E785.

8, Bödör, Cs., Alpár, D., Marosvári, D., Galik, B., Rajnai, H., Bátai, B., Nagy, Á., Kajtár, B., Burján, A., Deák, B., Schneider, T., Alizadeh, H., Matolcsy, A., Brandner, S., Storhoff, J., Chen, N., Liu, M.D., Ghali, N., Csala, I., Bagó G., A., Gyenesei, A., Reiniger L. Molecular subtypes and genomic profile of primary central nervous system lymphoma. Journal of Neuropathology and Experimental Neurology 2020, 79(2): 176–183.

9, Richárd Kiss, Gergő Papp, Szilvia Krizsán, Lili Kotmayer, Ambrus Gángó, Noémi Nagy, Bence Bátai, Zoltán Mátrai, Csaba Bödör, Donát Alpár. Screening for genomic copy number alterations in chronic lymphocytic leukemia using multiplex ligation-dependent probe amplification. [Hungarian] Hematológia-Transzfuziológia 2018, 51(1): 31-40.

DOI:10.14753/SE.2025.3134

10. ACKNOWLEDGEMENTS

I am grateful to Professor András Matolcsy, Head of the Department of Pathology and Experimental Cancer Research at Semmelweis University for welcoming me as a PhD student at the Department of Pathology and Experimental Cancer Research.

I owe special thanks to Professor Csaba Bödör, my PhD supervisor for not just leading our research projects at the Molecular Oncohematology Research Group, but providing scientific supervision, true mentoring, friendship and football companion throughout the years.

I would like to thank the current and previous members of the Molecular Oncohematology Research Group: Ambrus Gángó for introducing me to molecular diagnostics research, Noémi Nagy for showing how important accuracy is in research and Richard Kiss for showing skills in research management.
I would like to especially thank Ákos Nagy for the shared work, *long* projects and *long* hours together in the lab.
I am especially grateful to Gábor Bedics for teaching me how to exploit the power of bioinformatics and providing not just scientific input, but also emotional support when needed most.
I would like to thank Lili Kotmayer, Tamás László, Péterffy Borbála and Anna Bekő for creating an inspiring and vibrant atmosphere in the research group and for the best conferences together.
I would like to thank Luca Varga and Gabriella Szepesi for taking over all the running research projects when I finished my PhD studies and working on them since that with effort and accuracy I could not bear.
I would like to thank Richárd Hanza and Anna Udvari for contributing to research projects of the thesis and ongoing research projects and for teaching me through teaching.

I would also like to thank all the members of the Molecular Diagnostics Unit for being supportive of all research projects and teaching not just methods, but attitude to molecular diagnostics work as well. I am especially grateful to Stefánia Gróf, Luca Lévay, Adrienne

DOI:10.14753/SE.2025.3134

Bárányné Pallag, Lajos Hegyi, Erik Zajta and Róbert Horváth for their contribution in research projects.

I would like to thank all members of the Department of the Pathology and Experimental Cancer Research, especially the members of the Hematopathology Working Group for not just contributing to research, but also helping with scientific advice and mentoring. I owe special thanks to Ágota Szepesi for introducing me to the field of cutaneous lymphomas and together with Judit Csomor showing how to notice clinically interesting cases in the everyday's pathology practice.

I would like to thank the hungarian hematology community for providing samples and scientific input to our research projects and actively collaborating throughout the years. I would also like to thank the patients who were willing to take part in our studies and provided their samples to do molecular research.

I am also grateful to our international collaborators, who were sharing their invaluable knowledge and attitude through mutual research projects. I would like to especially thank Professor Jude Fitzgibbon who critically supervised our follicular lymphoma research projects throughout the years and gave me important lessons in *lege artis* scientific thinking.

Above all, I would like to thank my beloved wife, our children and all our families for supporting and loving me throughout the years of research.